PREPARATION OF PHOTO-ACTIVE ANTIBACTERIAL POLYLACTIC ACID FIBROUS MEMBRANES FOR FACEMASK APPLICATIONS

By

SASHA ECKSTEIN

THESIS

Submitted in partial satisfaction of the requirements for the degree of

MASTER OF SCIENCE

in

Biological Systems Engineering

in the

OFFICE OF GRADUATE STUDIES

of the

UNIVERSITY OF CALIFORNIA

DAVIS

Approved:

_____

Gang Sun, Chair

_____

Nitin Nitin

_____

Bruno Carciofi

Committee in Charge

2024

Acknowledgements

I would like to thank Dr. Gang Sun for being my thesis chair for my Master's degree. Thank you for your help and guidance since my junior year of undergraduate studies. You believed in my ability to help on this project. Thank you for the patience, encouragement, and understanding as I learned how to become a better researcher and scholar. Thank you for trusting me to help train and work with other students and colleagues.

I would also like to extend a thank you to my colleagues in the Gang Sung laboratory: Jiahan Zou, Noha Amaly, Yufa Sun, Bofeng Pan, Peixin Tang, Cunyi Zhao, and Shahid Islam. Thank you for teaching me the skills to become a better researcher and for all the help over the past few years. I would also like to acknowledge the help of my undergraduate researchers Lauren Defensor and Dara Baradaran for their help in running experiments.

I would further like to thank my collaborators from the University of Iowa and the University of Cincinnati: Dr. Sergey Grinshpun, Mr. Michael Yermakov, Ms. Xinyi Niu, Dr. Rui Li, and Dr. Guowen Song. Thank you for expanding my knowledge of how to test filtration materials as well as your help running the filtration efficiency experiments. It has been a wonderful experience being able to collaborate with other universities.

I would also like to thank all the University of California, Davis staff who have helped me along the way. Thank you to Molly Bechtel and Erin Friscia in the COE office for supporting me and my passion for the College of Engineering. Thank you to the staff in the Chemistry storeroom and the Scientific storeroom for all of the help sourcing materials. Thank you to Victor Duraj for the help with safety procedures and the yearly laboratory inspections.

I would like to acknowledge the financial support provided by the National Institute of Occupational Safety & Health (NIOSH)/Centers for Disease Control and Prevention (CDC) (R01 OH011947), Peter J. Shields and Henry A. Jastro Research and Student Support Awards and the 2023 AATCC Foundation Student Research Support Grant in helping me achieve my degree.

I would like to thank my friends and family for their support throughout this process. I am grateful for my friends here in Davis, Jiahan Zou, Kelly Graff, Nitya Raisinghani, Begum Koysuren, Camille King, as well as my friends away from Davis, Ella Caughey, Heather Childers, and many others. Thank you to my family for all the love and support: my parents (Janet Chin and Michael Eckstein), my grandmother (Bonnie Eckstein), and my siblings (Mia and Joseph Eckstein). A special thank you to my boyfriend Armen Nersiss for all the love, support, and encouragement during this process.

Abstract

Face masks or facial coverings are used to protect wearers from inhalation of pollutants, viruses, and particulate matter. Many face masks are single-use and made of petroleum-based polymers. Used facemasks may contain infectious viral particles on the surfaces, leading to concerns of plastic waste accumulation and risk of cross contamination. The development of reusable, biobased, biodegradable and biocidal filtration materials for use in face masks will reduce the environmental impact of personal protective equipment and reduce risks of cross contamination. Polylactic acid (PLA), a biobased and biodegradable polymer, was explored as an alternative to replace the current olefin polymers as a facemask filtration material. PLA was combined with an edible photosensitizer (menadione, VK3) and successfully electrospun into fibrous membranes. The physical properties of the materials were explored to determine its capabilities as a filtration material. The photoactivity of the membranes were assessed to determine its use as an antibacterial material. The PLA-VK3 membrane resulted in adequate filtering efficiency, generation of Reactive Oxygen Species (ROS), and antibacterial properties.

In this thesis, chapter 1 explores the benefits of face masks in preventing disease and the methodology behind filtration materials. It delves into the drawbacks and benefits of filtration materials used in face masks. It explores methods to decrease the environmental impact of face masks through the development of reusable, biocidal, biobased, and biodegradable filtration materials.

In chapter 2, the properties of filtration materials made from polylactic acid (PLA), a biobased, biodegradable thermoplastic polymer. PLA was successfully electrospun into nanofibrous membranes that provide adequate pressure drop and filtration efficiency for use in face masks. It also explores different alterations to the PLA membrane that could improve its performance, such as PLASMA treatment and the addition of photosensitizers.

In chapter 3, the use of a photosensitizer (VK3) as an antibacterial agent in PLA membranes was explored. VK3 was successfully electrospun with PLA to form an antibacterial filtration membrane. The VK3 within the membrane produces reactive oxygen species (ROS) under irradiation, which gives the

membranes an antibacterial effect. The mechanical and physical properties of the membranes are also discussed to determine the connection between the material and its filtration properties.

Chapter 4 provides a conclusion of the findings of PLA-VK3 electrospun membranes as new filtration material in face masks.

List of Figures

List of Tables

Table of Contents

Chapter 1. Introduction and Literature Review

1.1 Background

Throughout history, people have developed systems to protect themselves from imminent threats. These systems include protective gear to reduce injury during wartimes, camouflage to reduce detection of other people or animals or having someone stand watch at night. Today, disease is an imminent threat. Diseases and pathogens can be transferred between people, animals, and food sources through airborne, foodborne, and surface transmission routes. There are a variety of ways to protect oneself from disease such as washing hands, isolating from contacts with others, or covering respiratory paths to reduce the transmission of viral particles. Personal protective equipment (PPE) like face masks or gowns are used to protect the user from infection. During the global Coronavirus Disease 2019 (COVID-19) pandemic, governments around the world encouraged or mandated the use of the masks, to prevent the spread of COVID-19 and to reduce the strain on healthcare systems, which consequently increased the use of face masks outside of healthcare systems. A mask prevents the transfer of viral particles by stopping the exhalation of viral particles from an infected person and blocking the inhalation of the infectious particles by others. The use of facemasks is effective in reduction of the respiratory infections, if employed properly. Residual microbial droplets and particles on the surface of the used masks can be easily transmitted to the people who are in contact with them or can be aerosolized again by exhaled air, leading to cross-contamination and increased risk of infection [Bandyopadhyay, S., 2020]. One of the most impacted populations during a pandemic or flu season is healthcare workers, who are exposed to infectious particles in their working environment [Bandyopadhyay, S., 2020; Verbeek, J., 2016; Tian, C., 2022].

There are a variety of different face masks on the market, including surgical masks, N95 respirators, and fashion face masks. Surgical masks and N95 respirators are personal protective equipment providing different protection levels. Typically, surgical face masks protect against large

droplets, splashes, or sprays of bodily or other hazardous fluids. In comparison, N95 respirators, are not resistant to oil (N), provide a higher level of protection by blocking at least 95% particles as small as 0.3 microns in diameter [NIOSH, 1996]. During the pandemic, single-use surgical masks and N95 respirators were recommended to protect wearers from infection of COVID-19. These masks are intended to be used once and to be disposed of. Masks employ 2 different types of filtering mechanisms: depth filters and membrane filters [El-Atab, N., 2022]. A depth filter relies on multiple layers of filtering material to trap any viral particles or contaminants, whereas membrane filters rely on their fibrous structure to capture a larger size range of particles [El-Atab, N., 2022; Eudailey WA., 1983].

Many membrane filters are made from nanofibers, which are typical in the size range of less than 1 micron [Grafe, T., 2003]. Common methods of fabricating nanofibrous membranes include electrospinning, meltblowing, spun-bond, and wet spinning [Lim, H., 2010; Mcculloch, J., 2002; Suntech Textile Machinery, 2022; Rohani Shirvan, A., 2022]. Electrospinning, one of the representative manufacturing processes of nanofibrous membrane, uses an electric field to pull polymer solutions from a syringe into micro/nanofibrous fibers. This method allows the user to tune the fiber size based on the setup parameters [Kadam, V., 2021; Ostheller, M., 2023]. Electrospun nanofibers' large pore size and high surface area to volume ratio create membranes that are breathable and can filter sub-micrometer particulate matter [Wang, Z., 2021a; Alvarez Chavez, B., 2022].

The most common masks (surgical masks, N95 respirators) are made from melt blown polypropylene (PP), a thermoplastic polymer derived from petroleum. PP is used due to its piezoelectric properties, processability, and low price per kg ($1.25-$2.53/kg) [Ostheller, M., 2023; Alvarez Chavez, B., 2022]. Currently N95 respirators are made up of electrostatically charged meltblown polypropylene (PP) membranes. The charged PP attracts small particles and viral particles to the surface of the fibers preventing inhalation into the respiratory system [Omnexus, 2020; Hyperphysics, 2020]. N95 respirators have a limited shelf life due to the dissipation of the charge in PP. After the charge dissipates, the depth filtering mechanism still stops particles from reaching the respiratory system, but the ability to stop smaller particles is reduced.

The improper disposal of masks leads to the release of microplastics (MP) into aquatic and terrestrial environments. Plastics break down into microplastics, pollutants, or can become a place for microorganism and algae growth [Celik, S., 2023; Pizarro-Ortega, C., 2022; Sun, J., 2021; Cao, J., 2023]. Plastics like polypropylene undergo physical and chemical degradation after disposal, leading to changes in their material properties (hydrophilicity, crystallinity, chemical composition) [Pizarro-Ortega, C., 2022]. PP has low stability under oxidative environment, causing it to degrade when exposed to UV irradiation [Kadam, V., 2021]. The fibrous nature of filtration materials allows it to be easily broken down into microplastics [Celik, S., 2023; Pizarro-Ortega, C., 2022; Sun, J., 2021; Cao, J., 2023]. MPs can be released from filtration materials during use, sterilization, and disposal. Once MPs are released to the environment, they can accumulate in aquatic or terrestrial environments further posing environmental issues. MPs in aquatic environments can be toxic to marine life like the Marine Copepod *Tigriopus japonicus* [Sun, J., 2021]. Since MPs have been found in aquatic systems, there is a risk of ingestion by humans if MP laced aquatic animals are consumed. MPs have been found in human tissues, but the long-term toxicity and health implications of MPs are not fully understood [Celik, S., 2023]. One study found that the ingestion of MPs to the respiratory system can lead to respiratory issues such as asthma and lung disease [Cao, J., 2023]. Another risk of plastics breaking down is the production of pollutants directly affecting human health. Plastics can be broken down into phthalate esters, which are endocrine disruptors that enter humans via skin contact and inhalation [Cao, J., 2023]. This group of chemicals is known to decrease female fertility, increase allergies in children, and have links to obesity [Cao, J., 2023]. With the large number of single-use masks disposed of during and following the COVID-19 pandemic, the risk of ingesting pollutants such as phthalate esters increases. Research groups are exploring the risk of MP inhalation from wearing face masks. Both Li *et al.* and Cao *et al.* showed that MPs are released from masks during normal breathing cycles [Li, L., 2021; Bhangare, R., 2023]. Li *et al.* reported a much higher accumulation of MPs than Cao *et al*, which could be attributed to the unknown concentration of MP in the surrounding testing environment. Despite the risk of MP inhalation during face mask use, face masks

provide significant protection against infection. Users of single-use face masks should consider both the environmental risk upon disposal and the health risks associated with infection without using PPE.

To mitigate environmental damage, improvements to masks need to be made, including activities to manage disposal of face masks, extend the recommended usage time of masks, increase the number of uses, and enhancing protection against pathogens. Varghese *et al.* developed a method of recycling nonwoven polypropylene by blending it with acrylonitrile butadiene rubber to create a material with enhanced properties [Varghese, P. J G., 2022]. This removes face masks from waste streams, while creating a value-added product. To delay face masks from entering waste streams, masks can be reused after proper decontamination steps are taken to reduce the risk of cross contamination and infection. Decontamination strategies include sterilization by UV irradiation, vaporized hydrogen peroxide, sunlight exposure, hot water decontamination, and alcohol disinfection [Li, L., 2021; Boškoski, I., 2020; Rowan, N., 2020; Hossain, E., 2020; Juang, P., 2020; Wang, D., 2020]. However, after disinfection, N95 respirators could lose the electrostatic charge that enables them to filter smaller particulate matter than standard PP-based surgical masks. Since the filtration function of N95 respirators is dependent on the charge of the fibers, the material can be recharged by redepositing the electric charge on surface [Hossain, E., 2020; Juang, P., 2020; Juang, P., 2020]. A portion of the charge (~60%) can be redeposited on the surface by leaving the mask in open air to dry, and up to 90% of the original charge can be redeposited if the mask is dried with a hair dryer [Juang, P., 2020; Wang, D., 2020]. Reusable masks with removable filtering membranes are under development to reduce the amount of waste produced by PPE [El-Atab, N., 2022; Byrne, J., 2020]. The injection molded autoclavable, scalable, conformable (iMASC) system features a silicon mask designed to hold removable filtering membranes. These membranes can be detached, allowing the mask to be sterilized through autoclaving [Byrne, J., 2020]. These methods of recycling and reusing masks can help decrease the number of single-use plastics entering waste streams.

Since there are environmental risks and potential health risks associated with single-use PP based face masks, it is important to explore biobased, biodegradable alternatives. These alternatives would reduce the risk of MP production upon disposal and reduce the reliance on petroleum-based materials.

One group of biobased alternatives uses polysaccharide polymers directly derived from biomass and fibers, such as cellulose based compounds, wheat gluten, silk fibroins, gelatin, mycelium, and starch, to create filtration material [Kadam, V., 2021; French, V., 2023; Das, O., 2020; Pandit, P., 2021; Tang, P., 2020; Woranuch, S., 2017]. French *et al.* grew Pleurotus ostreatus (mycelium) on the surface of a layer of PP non-woven material to create a hydrophobic filtration layer to replace the PP middle layer of masks [French, V., 2023]. The addition of the mycelium layer increased the filtration efficiency to up to 97% depending on how long the mycelium grew on the surfaces. This reduces the need for multiple layers of PP to provide adequate protection against inhalation of viral particles. Kadam *et al.* developed gelatin/ β–cyclodextrin based nanofibrous membranes as low cost, biobased filtration material for capturing volatile organic compounds [Kadam, V., 2021]. The membranes had a high filtration efficiency (99% for particles <0.3 micronmeters), and were able to adsorb xylene, benzene, and formaldehyde. Das *et al.* and Pandit *et al.* explored the use of wheat biopolymers, a byproduct of the cereal industry, to create biobased, biodegradable face masks [Das, O., 2020; Pandit, P., 2021]. Wheat gluten biopolymers can be combined with lanosol and electrospun to create a flame retardant, biobased filtration material [Das, O., 2020]. Cotton-based masks are depth filters that provide ~70% protection from particulate matter [Pandit, P., 2021]. The addition of herbal additives or dyes to cotton face masks improved the antiviral properties of the masks thus reducing the risk of cross contamination [Pandit, P., 2021; Tang, P., 2020]. Pandit *et al.*, explored the use of herbal extracts to provide additional antifungal, antiviral, and antibacterial properties to cotton-fiber masks [Pandit, P., 2021]. Tang *et al.* explored the addition of anionic photosensitizers to cotton to create a biocidal cotton fabric that is antiviral and antibacterial in nature [Tang, P., 2020]. Plant based materials can be combined with thermoplastic polymers to create filtration materials with lower environmental impacts than pure PP based filtration materials. Woranuch *et al.* combined rice flour and polyvinyl alcohol (PVA) with silver nanoparticles (AgNP), NaOH, and β-cyclodextrin to create an antibacterial, biodegradable nanofibrous membrane [Woranuch, S., 2017]. PVA is a biodegradable synthetic thermopolymer that can be electrospun into nanofibrous membranes. The addition of rice flour to PVA decreased the reliance on PVA, a non-biobased polymer, while still allowing for adequate

filtration efficiency and pressure drop. The AgNP's provided antibacterial function by releasing Ag+ ions that interact with bacterial cells.

Cellulose based materials provide a highly renewable, biobased, biodegradable, biocompatible, and low-cost alternative to PP based filtration materials [Sharma, P., 2023, Stanislas, T., 2022, Garcia, R., 2022, Deng, C., 2022, Jonsirivilai, B., 2022]. Cellulose fibers were combined with antimicrobial additives such as polyhexamethyleneguanidine and neomycin sulfate, fingerroot extract, and AgNP's to create filtration materials with antibacterial properties [Deng, C., 2022, Jonsirivilai, B., 2022, Wang, Z., 2021b]. Jonsirivilai *et al.* combined bacterial cellulose with fingerroot extract, a medicinal plant with antibacterial, antiviral, and wound healing properties, to create an antibacterial filtration membrane [Jonsirivilai, B., 2022]. A large limitation to the use of cellulose based fiber is the cost to manufacture the fibers at a large scale [Sharma, P., 2023]. Despite the challenges, cellulose remains a renewable resource that could be harnessed to decrease reliance on petroleum-based products.

Silk fibroins (SF) can also be used to make filtration materials, and they provide a biobased, biodegradable, hydrophilic alternative to PP-based face masks. Wang *et al.* harnessed the hydrophilic properties of silk fibroins in combination with AgNP's to create an antimicrobial filtration membrane [Wang, Z., 2021b]. The hydrophilicity of SFs allowed for moisture and Ag+ ions to move throughout the membrane. Bacteria and viruses in the presence of Ag+ ions experienced oxidative stress which leads to cell damage and cell death. Wang *et al.* combined SF with $LiNbO_2$ nanoparticles and graphitic carbon nitride to create antibacterial nanofibrous membranes with high filtration efficiency and high levels of biocompatible [Wang, Z., 2021a]. These materials harnessed the hydrophilicity of silk fibroins and allowed it to generate electric charge, which is the mechanism that enhances PP's filtration efficiency in N95 respirators [Eudailey WA., 1983; Wang, Z., 2021a; Omnexus, 2020]. Polysaccharide based polymers are a viable option for replacing single-use PP masks to decrease environmental impact.

Another alternative to PP is to manufacture filtration materials out of polyester-based bioplastics. The use of biobased thermoplastic polymers such as polylactic acid (PLA), cellulose acetate, polybutylene succinate (PBS)prevents the production of MPs and pollutants upon mask disposal [Alvarez

Chavez, B., 2022; Morinval, A., 2022]. Due to the thermoplastic nature of these polymers, they could be meltblown or electrospun into fibrous membranes. Wang *et al.* explored electrospinning reusable, biodegradable filtration membranes made of cellulose acetate/thermoplastic polyurethanes enhanced with lithium chloride [Wang, J., 2022]. This filtration membrane displayed a filtration efficiency of up to 99.8% and a pressure drop of 52 Pa, leading to a breathable material that protects the user from particle inhalation. Ostheller *et al*. explored melt electrospinning of PBS into fibrous membranes for filtration applications [Ostheller, M., 2023]. PBS is a biodegradable, biobased polymer that is chemically resistant and able to be melt processed. Research on PBS fibrous membranes are less extensive compared to the studies on the electrospinning of polylactic acid (PLA).

PLA is a biobased, biodegradable thermoplastic polymer manufactured from lactic acid. Sugars in agricultural feedstocks can be broken down into lactic acid, which is then converted into PLA through fermentation or chemical synthesis [Lim, L., 2008; Singhvi, M., 2019; Li, G., 2020]. PLA can be industrially composted back into lactic acid after disposal [Maragkaki, A., 2023]. PLA has been extensively researched in the field of alternative membranes for face masks via electrospinning [Shao, W., 2023; Zhao, Y., 2024; Wang, L., 2022]. It has been successfully electrospun into nanofibrous membranes with optimal pressure drop and filtration efficiency for use in face masks.

As mentioned above, face masks protect the users from respiratory infections during a pandemic or a flu season by blocking infectious particles by entering the respiratory system. But residual bacteria or viral particles on the surface may survive and be further transmitted via contact or aerosolization leading to risks of cross-contamination. Mills *et al*. proposed the enzyme functionalized membranes to deactivate Severe Acute Respiratory Syndrome Coronavirus 2 (SARS-CoV-2, the specific viruses trended during COVID-19) when it reached the surface of the membrane [Mills, R., 2022]. By deactivating SARS-CoV-2 on the surface of the membrane, it reduced the risk of infection and cross-contamination. This decontamination method is effective for targeting a specific protein, making it useful during pandemics to isolate certain viruses or bacteria. However, it’s high specification is a drawback. If the targeted virus mutates, the method loses its effectiveness.

Another method of reducing cross contamination risk is the addition of antimicrobial compounds to face masks. These compounds do not target a specific microbe. Instead, they interact with the DNA and cell walls of microbes to kill the microbe. Some antimicrobial compounds explored include copper oxide nanoparticles (CuO), graphene oxide, zinc oxide (ZnO), AgNP, titanium dioxide (TiO_2), and photosensitizers [Wang, Z., 2021b; Ahmed, M., 2020; Ji, S., 2021; Pokhum, C., 2018; Naz, S., 2023; Minh Dat, N., 2021; Dat, N., 2022; Aydin-Aytekin, D., 2022; Liu, J., 2017; Nagar, V., 2022]. Ahmed *et al.* proposed combining CuO nanoparticles and graphene oxide with PLA and cellulose acetate to create an antimicrobial filtering material [Ahmed, M., 2020]. Both CuO nanoparticles and graphene oxide have antiviral activity decreasing the risks of cross-contamination. Another nanoparticle that has been explored for its antimicrobial nature is ZnO. Under light irradiation, ZnO forms Zn^{2+} ions, which upon contact with viral or bacterial particles, induces oxidative stress, resulting in cell death or damage. ZnO nanoparticles and AgNP can be incorporated into filtrating materials to give the membranes antibacterial functionality [Ji, S., 2021; Pokhum, C., 2018]. Ji *et al.* explored a layer filtration material with one layer of electrospun polyacrylonitrile (PAN) with ZnO nanoparticles and a layer of electrospun PAN with AgNP's with improve air filtration [Ji, S., 2021]. Pokhum *et al.* discussed the addition a coating of silver (Ag) and ZnO nanoparticles onto a nonwoven air filter [Pokhum, C., 2018]. The addition of Ag/ZnO nanoparticles helped to purify the air and remove particulate matter from the air.

Nanoparticles provide antimicrobial function due to their ability to form ions and high surface area, but the risks of nanoparticle dissipation and migration over time should be further explored. Nanoparticles in face masks can be inhaled and easily enter the respiratory system due to their small size. It has already been shown that MPs (<5 mm) can impose health risks after inhalation, and nanoparticles (<100 nm) are smaller than MPs which could pose future health risks [Cao, J., 2023]. There have been studies into the toxicity of ZnO [Liu, J., 2017; Nagar, V., 2022]. Zn+ was released on the surface of ZnO doped membranes and interacted with microbes, killing them via oxidative stress [Liu, J., 2017]. This protected the user from microbes but were potentially dangerous if the nanoparticles dislodged and entered the respiratory system. Nanoparticles have different toxicity depending on the size of the

nanoparticle used, as shown by Liu *et al.* [53]. It was found that ZnO nanoparticles have toxic effects on the SHSY5Y (neurological cells) cell line at smaller sizes (<100 nm, surface area 10-25 m2/g) [Liu, J., 2017]. At low quantities, ZnO is not shown to be toxic to mammalian cells, but with extended exposure and potential accumulation there could be greater risks [Nagar, V., 2022]. Since the exposure limits of nanoparticles are still under investigation, it is crucial to research antibacterial agents that are naturally occurring or naturally derived.

Photosensitizers are compounds that can be photoactivated to produce Reactive Oxygen Species (ROS). Organic photosensitizers produce ROS that can cause direct damage to DNA, lipids and proteins in microbes [Zhang, Z., 2020]. There are two possible mechanisms of ROS production from photosensitizers: Type I and Type II, as seen in Figure 1.1. In both types, the photosensitizer is excited from a ground state to a singlet excited state which undergoes intersystem crossing to a triplet state during irradiation. Then, ROS species are produced by the triplet excited molecule via a hydrogen abstraction from a polymer or a media (Type I) or collision with triplet oxygen ($^3O_2$) in air (Type II). Type I photosensitizers produce hydrogen peroxide (H_2O_2), hydroxyl radicals (OH·), or superoxide ($O_2^{-\cdot}$) as dominating ROS, whereas Type II photosensitizers produce singlet oxygen ($^1O_2$) dominantly [Zhang, Z., 2020; Schnabel, W., 2014; Zhang, Z., 2021]. Previous studies have shown that vitamins and their derivatives could generate ROS under daylight or UVA irradiation. Potential photosensitizers include menadione (VK3), VB2, Rose Bengal, and curcumin [Tang, P., 2020; Zhang, Z., 2019; Dias, L., 2020; Zhang, Z., 2020; Schnabel, W., 2014; Zhang, Z., 2021]. The produced ROS have cytotoxicity to a variety of different microbes including *E. coli* [56-69]. Among these vitamin derivatives, menadione (vitamin K3, VK3) could generate multiple ROS species, including $^1O_2$ and OH· efficiently, which interact with the cell membrane of microbes and increase the oxidative stress on the microbe. The increased concentration of ROS on the outside of the cells leads to cell rupture. One limitation of using photosensitizers as antimicrobial agents is the transient existence of ROS, with OH· and $^1O_2$ having half-lives of 10^{-6} seconds and 10^{-9} seconds, respectively [Rubio, C., 2021; Andrés Juan, C., 2021; Das, K., 2014]. Consequently, the photosensitizers need to be in immediate proximity to the microbe; otherwise, the ROS will dissipate

before the virus or bacteria is killed. The benefit of using photosensitizers is that there are many naturally derived and naturally occurring photosensitizers, such as curcumin and menadione [Dias, L., 2020; Zhang, Z., 2020].

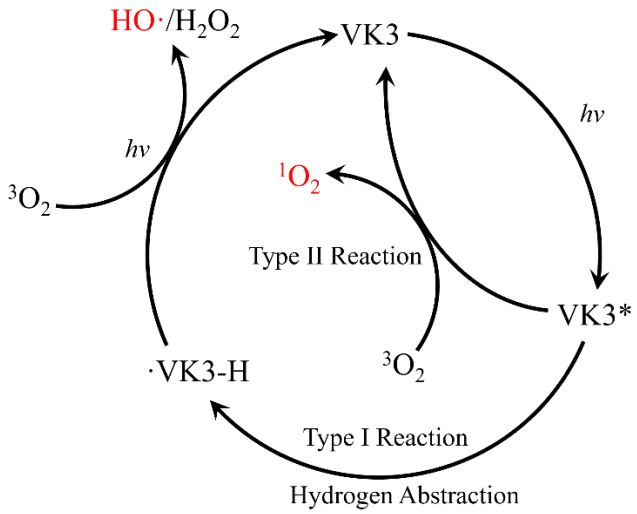

Figure 1.1. Photosensitizer mechanism displaying type I and type II photosensitizers.

This research intends to reduce the concerns regarding the use of nanoparticles by using a vitamin derivative photosensitizer to provide antimicrobial properties. The addition of menadione allows the material to provide light-induced biocidal ROS without using any nanoparticles. Besides, the electrospun nanofibrous membrane PLA membrane will be used as a layer in a face mask. By electrospinning a fibrous membrane of biodegradable PLA and VK3, we can produce a biobased, biodegradable, and antibacterial face mask material for future applications.

1.2 Research Objectives

After reviewing literature, it was decided to explore the use of PLA in combination with VK3 as an antimicrobial agent to create a biodegradable and biocidal filtration material. Electrospinning is employed as a promising laboratory scale method to create membranes with small fiber sizes and fibrous membrane mimicking the facemask filtering materials.

Research Objectives:

1. Fabrication of nanofibrous membranes from biobased polymers and photo-active antimicrobial compounds via electrospinning processes.
2. Evaluate filtration properties and air permeability of the material for use in respirators.
3. Evaluate antibacterial properties of the nanofibrous membranes under daylight exposure.

Objective 1 was achieved by combining PLA and VK3 in solution and electrospinning that solution into fibrous membranes. The exploration of PLA dissolution and electrospinning is discussed in Chapter 2. To evaluate the electrospinnability of, PLA was dissolved in a variety of solvent to achieve homogenous solutions. Upon successful dissolution, the solutions were used in an electrospinning setup to create fibrous membranes. The membranes were initially spun without addition of menadione to determine the ideal electrospinning conditions for a PLA solution. A 4:1 mixture of dichloromethane (DCM) to dimethylformamide (DMF) was identified as a proper solvent system for electrospinning of PLA, resulting in fibrous membranes in good morphologies conditions.

Objective 2 was explored in both Chapter 2 and Chapter 3, which examined the filtration efficiency and the pressure drop across PLA fibrous membranes sandwiched between two layers of spunbond PLA membranes. Several membranes displayed pressure drop and filtration efficiency that met U.S. National Institute for Occupational Safety and Health (NIOSH) guidelines for facemask materials, positioning them as suitable alternatives to existing filtration materials.

Objective 3 was achieved by the addition of VK3 to the PLA fibrous membranes. The feasibility to electrospin VK3 with PLA is briefly discussed in Chapter 2, showing that it is feasible to electrospin VK3 and PLA in one system. To determine if the electrospun PLA-VK3 membranes are suitable for use as biocidal filtration membranes, the production of ROS on the PLA-VK3 fibrous membranes was measured, and the corresponding antibacterial properties were characterized. The production of ROS was tested under UVA (315 nm- 400 nm) and D65 (300 nm – 800 nm). After the initial ROS production was discovered, photoactive functions of the PLA-VK3 membranes were found highly unstable and difficult

to control over time. Thus, a study was conducted characterizing the extended storage stability of the photoactive functions of PLA-VK3 nanofibrous membranes. The surface bound VK3 might be affected by both oxygen and light exposure. Thus, the storage conditions of in the dark and with reduced oxygen exposure were utilized in the study. The ROS production was monitored weekly to access if the stability of VK3 when exposed to oxygen. Given that the intended use of the materials is in hospitals, the samples were also subjected to lighting conditions that simulate a hospital room to evaluate how light exposure might alter the material's antibacterial properties. These tests showed that the stability of the VK3 in the PLA-VK3 membranes was limited.

1.3 References

Alvarez Chavez, B., Raghavan, V., Tartakovsky, B., A comparative analysis of biopolymer production by microbial and bioelectrochemical technologies. *RSC Advances*, (2022), 16105-16118, 12(25)

Ahmed, M., Afifi, M., Uskoković, V., Protecting healthcare workers during COVID-19 pandemic with nanotechnology: A protocol for a new device from Egypt. *Journal of Infection and Public Health*, (2020), 1243-1246, 13(9)

Andrés Juan, C., Manuel Pérez del la Lastra, J., Plou F., et al., Molecular Sciences The Chemistry of Reactive Oxygen Species (ROS) Revisited: Outlining Their Role in Biological Macromolecules (DNA, Lipids and Proteins) and Induced Pathologies. *International Journal of Molecular Sciences*, (2021), 4642, 22

Aydin-Aytekin, D., Gezmis-Yavuz, E., Buyukada-Kesici, E., et al., Fabrication and characterization of multifunctional nanoclay and TiO2 embedded polyamide electrospun nanofibers and their applications at indoor air filtration. *Materials Science and Engineering B*, (2022), 279

Bandyopadhyay, S., Baticulon, R., Kadhum, M., et al., Infection and mortality of healthcare workers worldwide from COVID-19: A systematic review. *BMJ Global Health*, (2020), 5(12)

Bhangare, R., Tiwari, M., Ajmal, P., et al., Exudation of microplastics from commonly used face masks in COVID-19 pandemic. *Environmental Science and Pollution Research*, (2023), 35358-35268, 30(12)

Boškoski, I., Gall, C., Wallace, M., et al., COVID-19 pandemic and personal protective equipment shortage: protective efficacy comparing masks and scientific methods for respirator reuse. *Gastrointestinal Endoscopy*, (2020), 92(3)

Byrne, J., Wentworth, A., Chai, P., et al., Injection Molded Autoclavable, Scalable, Conformable (iMASC) system for aerosol-based protection: A prospective single-arm feasibility study. *BMJ Open*, (2020), 10(7)

Cao, J., Shi, Y., Yan, M., et al., Face Mask: As a Source or Protector of Human Exposure to Microplastics and Phthalate Plasticizers? *Toxics*, (2023), 11(2)

Celik, S., The Release Potential of Microplastics from Face Masks into the Aquatic Environment. *Sustainability (Switzerland)*, (2023), 15(19)

Das, K., Roychoudhury, A., Reactive oxygen species (ROS) and response of antioxidants as ROS scavengers during environmental stress in plants. *Frontiers in Environmental Science*, (2014), 2

Das, O., Neisiany, R., Capezza, A., et al., The need for fully bio-based facemasks to counter coronavirus outbreaks: A perspective. *Science of the Total Environment*, (2020), 736

Dat, N., Thinh, D., Huong, L., et al., Facile synthesis and antibacterial activity of silver nanoparticles modified graphene oxide hybrid material: the assessment, utilization, and anti-virus potentiality. *Materials Today Chemistry*, (2022), 23

Dias Cavalcante, A., Martinez, R., Mascio, P., et al., Cytotoxicity and mutagenesis induced by singlet oxygen in wild type and DNA repair deficient Escherichia coli strains. *DNA Repair 1*. (2002), 1051-1056

Dias, L., Blanco, K., Mfouo-Tynga, I., et al., Curcumin as a photosensitizer: From molecular structure to recent advances in antimicrobial photodynamic therapy. *Journal of Photochemistry and Photobiology C: Photochemistry Reviews*, (2020), 45

Deng, C., Seidi, F., Yong, Q., et al., Antiviral/antibacterial biodegradable cellulose nonwovens as environmentally friendly and bioprotective materials with potential to minimize microplastic pollution. *Journal of Hazardous Materials*, (2022), 424

El-Atab, N., Mishra, R., Hussain, M., Toward nanotechnology-enabled face masks against SARS-CoV-2 and pandemic respiratory diseases. *Nanotechnology*, (2022), 33(6)

Eudailey WA. Membrane filters and membrane-filtration processes for health care. *Am J Hosp Pharm*. 1983 Nov;40(11):1921-3. PMID: 6650520.

French, V., Du, C., Foster, E., Mycelium as a self-growing biobased material for the fabrication of single layer masks. *Journal of Bioresources and Bioproducts*, (2023), 399-407, 8(4)
Garcia, R., Stevanovic, T., Berthier, J., et al., Cellulose, Nanocellulose, and Antimicrobial Materials for the Manufacture of Disposable Face Masks: A Review. *BioResources*, (2022), 4321-4353, 16(2)
Grafe, T., Graham, K., Polymeric Nanofibers and Nanofiber Webs: A New Class of Nonwovens (2003)
Hossain, E., Bhadra, S., Jain, H., et al., Recharging and rejuvenation of decontaminated N95 masks. *Physics of Fluids*, (2020), 32(8)
Dielectric Constants at 20°C. *HyperPhysics*. Accessed: 12 Dec 2020
Differences Among Spunbond and Meltblown Nonwoven. *Suntech Textile Machinery*, (2022) Date Accessed: 28 April 2024
Jonsirivilai, B., Torgbo, S., Sukyai, P., Multifunctional filter membrane for face mask using bacterial cellulose for highly efficient particulate matter removal. *Cellulose*, (2022), 6205-6218, 29(11)
Juang, P., Tsai, P., N95 Respirator Cleaning and Reuse Methods Proposed by the Inventor of the N95 Mask Material. *Journal of Emergency Medicine*, (2020), 817-820, 58(5)
Ji, S., Tiwari, A., Oh, H., et al., ZnO/Ag nanoparticles incorporated multifunctional parallel side by side nanofibers for air filtration with enhanced removing organic contaminants and antibacterial properties. *Colloids and Surfaces A: Physicochemical and Engineering Aspects*, (2021), 621
Kadam, V., Truong, Y., Schutz, J., et al., Gelatin/β–Cyclodextrin Bio–Nanofibers as respiratory filter media for filtration of aerosols and volatile organic compounds at low air resistance. *Journal of Hazardous Materials*, (2021), 403
Li, L., Zhao, X., Li, Z., et al., COVID-19: Performance study of microplastic inhalation risk posed by wearing masks. *Journal of Hazardous Materials*, (2021), 411
Li, G., Zhao, M., Xu, F., et al., Synthesis and Biological Application of Polylactic Acid, *Molecules*, (2020), 25(21)
Lim, H., A Review of Spun bond Process. *Journal of Textile and Apparel, Technology and Management*, (2010), 6(3)
Lim, L., Auras, R., Rubino, M., Processing technologies for poly(lactic acid). *Progress in Polymer Science (Oxford).* (2008), 820-852, 33(8)
Liu, J., Kang, J., Yin, S., et al., Zinc oxide nanoparticles induce toxic responses in human neuroblastoma SHSY5Y cells in a size-dependent manner. *Internation Journal of Nanomedicine*, (2017), 8085 8099, 12
Maragkaki, A., Malliaros, N., Sampathianakis, I., et al., Evaluation of Biodegradability of Polylactic Acid and Compostable Bags from Food Waste under Industrial Composting. *Sustainability (Switzerland)*, (2023), 15(22)
Mcculloch, J., The History of the Development of Melt Blowing Technology. *International Nonwovens Journal*. (2002)
Mills, R., Vogler, R., Bernard, M., et al., Aerosol capture and coronavirus spike protein deactivation by enzyme functionalized antiviral membranes. *Communications Materials*, (2022), 3(1)
Minh Dat, N., Tan Tai, L., Tan Khang P., et al., Synthesis, characterization, and antibacterial activity investigation of silver nanoparticle-decorated graphene oxide. *Materials Letters*, (2021), 285
Morinval, A., Averous, L., Systems Based on Biobased Thermoplastics: From Bioresources to Biodegradable Packaging Applications. *Polymer Reviews*, (2022), 653-721, 62(4)
Munna, M., Influence of Exogenous Oxidative Stress on Escherichia Coli Cell Growth, Viability and Morphology. *American Journal of Bioscience*, (2013), 59, 1(4)
Naz, S., Gul A., Zia, M., et al., *Synthesis, biomedical applications, and toxicity of CuO nanoparticles. Applied Microbiology and Biotechnology*, (2023), 1039-1061, 107(4)
Nagar, V., Singh, T., Tiwari, Y., et al., ZnO Nanoparticles: Exposure, toxicity mechanism and assessment. *Materials Today: Proceedings*, (2022), 56-63, 69
NIOSH Guide to the Selection and Use of Particulate Respirators. The National Institute for Occupational Safety and Health (*NIOSH*). (1996)

Ostheller, M., Balakrishnan, N., Beukenberg, K., et al., Pilot-Scale Melt Electrospinning of Polybutylene Succinate Fiber Mats for a Biobased and Biodegradable Face Mask. *Polymers*, (2023), 15 (13)
Pandit, P., Maity, S., Singha, K., et al., Potential biodegradable face mask to counter environmental impact of Covid-19. *Cleaner Engineering and Technology*, (2021), 4
Pizarro-Ortega, C., Dioses-Salinas, D., Fernández Severini, M., et al., Degradation of plastics associated with the COVID-19 pandemic, *Marine Pollution Bulletin*, (2022), 176
Pokhum, C., Intasanta, V., Yaipimai, W., et al., A facile and cost-effective method for removal of indoor airborne psychrotrophic bacterial and fungal flora based on silver and zinc oxide nanoparticles decorated on fibrous air filter. *Atmospheric Pollution Research*, (2018), 172-177, 9(1)
Rohani Shirvan, A., Nouri, A., Sutti, A., A perspective on the wet spinning process and its advancements in biomedical sciences, *European Polymer Journal*. (2022) 181
Rowan, N., Laffey, J., Challenges and solutions for addressing critical shortage of supply chain for personal and protective equipment (PPE) arising from Coronavirus disease (COVID19) pandemic – Case study from the Republic of Ireland. *Science of the Total Environment*, (2020), 725
Rubio, C., Cerón, J., Spectrophotometric assays for evaluation of Reactive Oxygen Species (ROS) in serum: general concepts and applications in dogs and humans. *BMC Veterinary Research*, (2021), 17(1)
Schnabel, W., Visible and Ultraviolet Light. In Polymers and Electromagnetic Radiation, *W. Schnabel (Ed.)*. (2014)
Shao, W., Niu, J., Han, R., et al., Electrospun Multiscale Poly(lactic acid) Nanofiber Membranes with a Synergistic Antibacterial Effect for Air-Filtration Applications. *ACS Applied Polymer Materials*, (2023), 9632-9641, 5(11)
Sharma, P., Mittal, M., Yadav, A., et al., Bacterial cellulose: Nano-biomaterial for biodegradable face masks – A greener approach towards environment. *Environmental Nanotechnology, Monitoring and Management*, (2023), 19
Singhvi, M., Zinjarde, S., Gokhale, D., Polylactic acid: synthesis and biomedical applications. *Journal of Applied Microbiology*, (2019), 1612-1626, 127(6)
Stanislas, T., Bilba, K., de Oliveira Santos, R., et al., Nanocellulose-based membrane as a potential material for high performance biodegradable aerosol respirators for SARS-CoV-2 prevention: a review. *Cellulose*, (2022)
Sun, J., Yang, S., Zhou, G., et al., Release of Microplastics from Discarded Surgical Masks and Their Adverse Impacts on the Marine Copepod Tigriopus japonicus. *Environmental Science and Technology Letters*, (2021), 1065-1070, 8(12)
Tang, P., Zhang, Z., El-Moghazy, A., et al., Daylight-Induced Antibacterial and Antiviral Cotton Cloth for Offensive Personal Protection. *ACS Applied Materials and Interfaces*, (2020), 49442-49451, 12(44)
The Definitive Guide to Polypropylene (PP), *Omnexus*. Accessed: 11 Dec 2020
Tian, C., Lovrics, O., Vaisman, A., et al., Risk factors and protective measures for healthcare worker infection during highly infectious viral respiratory epidemics: A systematic review and meta analysis. *Infection Control and Hospital Epidemiology*, (2022), 639-650, 43(5)
Varghese, P. J G., David, D., Karuth, A., et al., Experimental and Simulation Studies on Nonwoven Polypropylene-Nitrile Rubber Blend: Recycling of Medical Face Masks to an Engineering Product. *ACS Omega*, (2022), 4791-4803, 7(6)
Verbeek, J., Ijaz, S., Mischke, S., et al., Personal protective equipment for preventing highly infectious diseases due to exposure to contaminated body fluids in healthcare staff. *Cochrane Database of Systematic Reviews*. (2016), 2016(4)
Wang, D., Sun, B., Wang, J., et al., Can Masks Be Reused After Hot Water Decontamination During the COVID-19 Pandemic? *Engineering*, (2020), 115-1121, 6(10)
Wang, J., Liu, S., Yan, X., et al., Biodegradable and reusable cellulose-based nanofiber membrane preparation for mask filter by electrospinning. *Membranes*, (2022), 12(1)

Wang, L., Xiong, J, et al., Biodegradable and high-performance multiscale structured nanofiber membrane as mask filter media via poly(lactic acid) electrospinning. *Journal of Colloid and Interface Science*. (2022), 961-970

Wang, Z., Cui, Y., Feng, Y., et al., A versatile Silk Fibroin based filtration membrane with enhanced mechanical property, disinfection and biodegradability. *Chemical Engineering Journal*, (2021), 426

Wang, Z., Li, J., Shao, C., et al., Moisture power in natural polymeric silk fibroin flexible membrane triggers efficient antibacterial activity of silver nanoparticles. *Nano Energy*, (2021), 90

Woranuch, S., Pangon, A., Puagsuntia, K., et al., Starch-based and multi-purpose nanofibrous membrane for high efficiency nanofiltration. *RSC Advances*, (2017), 35368-35375, 7(56)

Zhang, Z., Si, Y. and Sun, G., Photoactivities of vitamin K derivatives and potential applications as daylight-activated antimicrobial agents. *ACS sustainable chemistry & engineering*, (2019) 18493 18504, *7*(22).

Zhang, Z., El-Moghazy, A.Y., Wisuthiphaet, N., et al., Daylight-induced antibacterial and antiviral nanofibrous membranes containing Vitamin K derivatives for personal protective equipment. *ACS Applied Materials and Interfaces*, (2020), 49416-49430, 12

Zhang, Z., Photochemical Study of Vitamin K and Vitamin B Derivatives and Their Applications as Photo induced Antimicrobial Agents. *Dissertation* (2021)

Zhao, Y., Ming, J., Cai, S., et al., One-step fabrication of polylactic acid (PLA) nanofibrous membranes with spider-web-like structure for high-efficiency PM0.3 capture. *Journal of Hazardous Materials*, (2024), 165

Chapter 2. Exploration of Electrospinning PLA

2.1 Abstract

The current facemasks are single-use, petroleum-based, and may still cause cross contamination after usage if improperly disposed of. N95 masks, a category of membrane filtration respirators, blocks greater than 95% of the particles due to their charged fibers, which can dissipate over time. Polylactic acid (PLA), a biobased and biodegradable polymer, was explored as an alternative to replace the current olefin polymers used in filtration material. PLA in solution was successfully electrospun to create fibrous membranes for utilization as a filtration layer within facemasks. The physical properties of the fibrous membrane were then explored to determine its capabilities as a filtration material. The PLA based membrane provides a sufficient particle collection efficiency (>80%) and pressure drop (<35 mm w.g. at 85 L/min) without being charged.

2.2 Introduction

Polylactic acid (PLA) is a thermoplastic biobased polymer alternative to olefin polymers. The uses of PLA include food packaging, tissue engineering, drug delivery, and surgical implants [Lim, L., 2008; Singhvi, M., 2019; Li, G., 2020; Lawal, U., 2023]. PLA has also been authorized for use in biomedical applications by the FDA, meaning that it is suitable to use inside of the body [Li, G., 2020]. In turn, it would also be appropriate to be used in filtration media that is in close contact with human bodies. PLA is made from lactic acid molecules, which are synthesized by breaking down sugars (glucose, starch) via fermentation or chemical synthesis [Lim, L., 2008; Singhvi, M., 2019; Li, G., 2020]. Agricultural wastes can serve as a feedstock to produce the lactic acid that is converted into PLA transforming the waste to a value-added product. PLA can be processed in a variety of different manufacturing methods from extrusion to injection molding to electrospinning [Lim, L., 2008; Singhvi, M., 2019; Li, G., 2020; Lawal, U., 2023; Shao, W., 2023; Zhao, Y., 2024; Wang, L., 2022; Liang, C., 2023; Selatile, M., 2020; Khatsee, S., 2018; Wang, S., 2019; Baji, A., 2020; Karabulut, F., 2021; Wu, J., 2022; Casasola, R., 2014]. Not only is PLA biobased; it is also biodegradable under industrial composting conditions [Maragkaki,

A., 2023]. During the composting process, PLA is broken down into lactic acid, which is naturally occurring in living things and can further be broken down into carbon dioxide and water. Due to its increasing usage at an industrial scale, PLA was chosen as the polymer for this study. It is dissolvable in solution and able to be electrospun into fibrous membranes [Shao, W., 2023; Zhao, Y., 2024; Wang, L., 2022; Liang, C., 2023; Selatile, M., 2020; Khatsee, S., 2018; Wang, S., 2019; Baji, A., 2020; Karabulut, F., 2021; Wu, J., 2022; Casasola, R., 2014]. Electrospun PLA membranes display similar filtration properties to polypropylene (PP) based face masks.

2.3 Experimental Methods

2.3.1 Materials

Polylactic acid 6202D (PLA) was produced by NatureWorks (Minneapolis, MN). Dichloromethane (DCM), dimethylformamide (DMF), dimethyl acetamide (DMAc), chloroform, tetrahydrofuran (THF), and menadione (VK3) were purchased from Sigma Aldrich (St. Louis, USA). *P*-Nitroso-*N*, *N*-dimethylaniline (*p*-NDA) was purchased from TCI Co. Ltd. (Tokyo, Japan). Phosphate Buffer Solution (PBS) 10X powder was purchased from Thomas Scientific LLC (PA, USA). All the chemicals and supplies were used as received without any further purification.

Over the course of my research, multiple electrospinning setups were used, as seen in Figure 2.1. For all the different setups, the solution injection speed was set at 1.5 mL/hr, the distance from the end of the needle to the collection device was set at 20 cm, 20 mL syringes and 18-gauge 1-inch cannula needles were used, and the voltage applied to the needles was set at 25 kV. The first electrospinning setup (ES#1), as seen in Figure 2.1a, used a collection device with a diameter of 16.5 cm and a length of 26.5 cm, which rotated at 10 rpm. The solution was placed into 4 separate syringes that were loaded into two NE 300 single syringe pumps (syringepump.com, USA). The second electrospinning setup (ES#2) employed the same collection device as ES#1, but an NE-1600 multichannel 6 syringe-pump (syringepump.com, USA) loaded with 6 syringes was used to hold the solutions (Figure 2.1b). All samples made by using ES#1 and ES#2 were spun onto wax paper and then dried at 40°C for 4-5 hours until they were able to be removed

from the wax paper. Electrospinning setup #3 (ES#3) includes the 6-syringe pump loaded with 2 syringes and a new collection device with a diameter of 9 cm and a length of 20 cm (Figure 2.1c). The pump was only loaded with 2 syringes to account for the change in size of the collection device. The speed of the collection device was set at 120 rpm. The smaller collection device reduced the amount of solution needed for electrospinning, which in turn helps to reduce the waste associated with the electrospinning process. Samples electrospun using ES#3 were also dried at 40°C for 4-5 hours until the solvent evaporated. For samples used in filtration efficiency tests, the samples were electrospun onto a layer of PLA spunbond nonwoven fabric (18g/m^2).

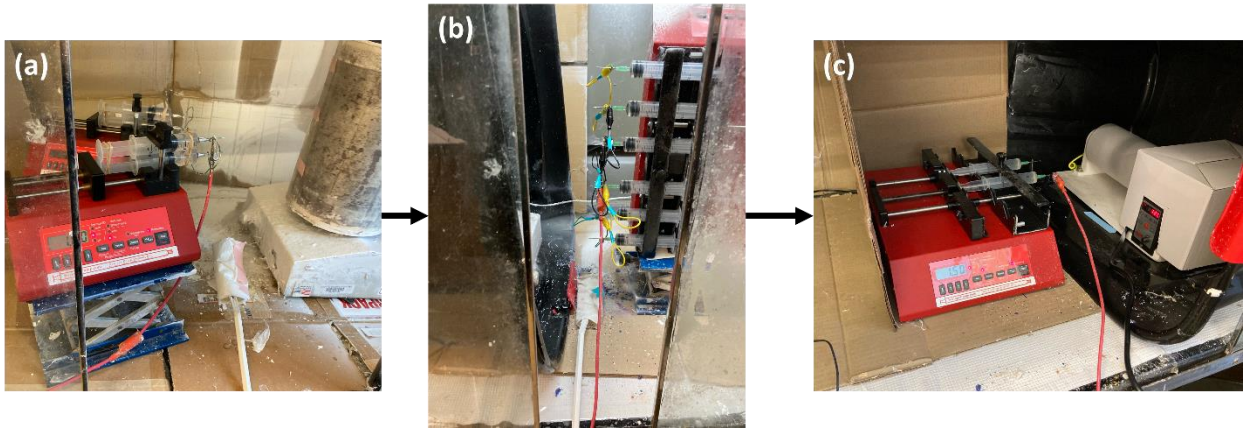

Figure 2.1. Electrospinning setups (a) ES#1 includes 2 single syringe pumps with 4 syringes and a large rotating collection device (b) ES#2 includes 1- 6 syringe multichannel pump loaded with 6 syringes and a large rotating collection device (c) ES#3 includes a 6-syringe multichannel pump and a small rotating collection device.

Polymer concentration in different solvent systems affect electrospinning process and quality of fibrous membranes, therefore multiple solvents and concentrations of PLA in solution were investigated. Solvents of DMF, DMAc and DCM were selected to prepare solvent mixtures for dissolution of PLA. For a 10 wt% PLA solution, 10 grams of PLA were added to 90 mL of the solvent, and for a 12wt% solution, 12 grams of PLA was added to 88 mL of the solvent. The PLA was dissolved in the solution overnight to ensure complete polymer dissolution before electrospinning. The amount of VK3 added to the PLA solution varied from 10% to 30% VK3 based on the solid in solution during initial tests of generation of reactive oxygen species (ROS) under light exposure. VK3 was added into the PLA solution in the day of

electrospinning to reduce potential oxidation. After electrospinning, the fibrous membrane samples were dried at 50°C for 4-5 hours to remove any residual solvent.

To alter the hydrophilicity of the membrane, oxygen plasma treatment of the membranes was employed. Oxygen plasma treatment could introduce hydroxyl groups on surfaces of PLA and increase the hydrophilicity of materials [Mozetič, M., 2020]. After the membrane samples containing VK3 were dried, they were cut into 10 mg samples and placed into a plasma cleaner (Harrick Plasma, Ithaca, NY, USA) for the plasma treatment. The samples were treated under vacuum for the allotted time frames and then exposed to oxygen to produce hydroxyl or other oxygen containing moieties on the surfaces of the membrane materials.

2.3.3 Material Characterization

Water contact angles of the membrane samples were determined to measure their hydrophilicity, which was conducted by dropping a droplet of water onto a 1cm x 1cm sample and measuring the water contact angle. Images of the water droplet were taken using a Dino-Lite Premier Digital Microscope (Taiwan). The fiber size and morphology of the PLA fibrous membranes were examined using a scanning electron microscope (SEM) (Thermo Fisher Quattro S Environmental SEM, USA). To determine the average fiber size and fiber size distribution, an ImageJ image processing software was employed with the use of the DiameterJ plug-in. To determine the tensile strength of the material, samples in size of 3.0 cm x 5.0 cm of each material were prepared and tested using an INSTRON 5566 universal tester following ASTM testing method D638.

2.3.4 Pressure Drop and Filtration Testing

Since the electrospun materials will be used as filtration materials for masks, the pressure drop across and filtration efficiency of the membrane were measured. The tests were conducted in a 24 m^3 aerosol exposure chamber (University of Cincinnati, Department of Environmental and Public Health Sciences). Sodium chloride (NaCl) polydisperse aerosol was generated using a particle generator (Model 8026, TSI Inc.). The PLA electrospun membranes were sandwiched between 2 layers of PLA nonwoven

fabrics to mimic a multilayered mask. The PLA samples were mounted in a square frame measuring 155 mm x 155 mm. The pressure drop across the membranes was measured with the Magnehelic differential pressure gage (Dwyer Instruments Inc., Michigan Citi, IN, USA). To measure the aerosol particle concentration a particle size-selectively with an electrical low-pressure impactor (ELPI; Dekati Ltd., Tampeer, Finland) was used. The equipment was placed into a Class II biosafety cabinet (SterilchemGard; Baker Company, Inc., Sanford, ME, USA). The filtration efficiency of η (%) and the pressure drop were determined using a particle size of 0.3 to 0.5 μm at 2 different air face velocities (30 L/min and 85 L/min).

2.3.5 Singlet Oxygen Testing

The amount of singlet oxygen ($^1O_2$) produced by the samples under light exposure was measured by using a 2-solution method [Zhang, Z., 2021; Zhang, Z., 2020; Islam, S., 2023; Sheng, L., 2020; Zhang, Z., 2019; Tang, P., 2020; Deng, Y., 2020; Kraijic, I., 1978; Herman, J., 2019]. Two separate solutions, *p*-NDA (50 μM) with L-histidine (0.01 M) in PBS and *p*-NDA (50 μM) without L-histidine in PBS, were prepared [Zhang, Z., 2020]. The *p*-NDA solution containing L-histidine reacts with both $^1O_2$ and hydroxyl radicals produced, bleaching the *p*-NDA in the solution [Kraijic, I., 1978]. The *p*-NDA solution without L-histidine is not able to react with $^1O_2$ but with hydroxyl radicals. A 10 mg electrospun fibrous membrane sample was immersed in 10 mL of each solution. The samples were irradiated under either D65 lighting for times between 0 and 60 minutes, respectively. The amount of *p*-NDA left in the solution was measured quantitatively with the absorbance at 440 nm with λ_{max} by a UV-vis spectrometer (Evolution 600, ThermoFisher Scientific, USA). To determine the relative singlet oxygen produced by the sample, the difference in concentrations between the solutions with L-Histidine and without L-histidine was determined following Equation 1 [Kraijic, I., 1978; Herman, J., 2019].

$$\Delta\Delta O.D. = (H_0 - H_1) - (P_0 - P_1) \quad (1)$$

Where H_0 = initial 50 µM *p*-NDA with L-histidine solution reading

H_1= 50 µM *p*-NDA with L-histidine solution reading after irradiation

P_0= initial 50 µM *p*-NDA solution reading

P_1= 50 µM *p*-NDA solution reading after irradiation

2.4 Results and Discussion

Initial testing was conducted to determine a proper solvent solution to be used for electrospinning. Different solvents, including DCM, DMF, DMAc, Acetone, Chloroform, and THF, were explored to dissolve PLA [Shao, W., 2023; Zhao, Y., 2024; Wang, L., 2022; Liang, C., 2023; Selatile, M., 2020; Khatsee, S., 2018; Wang, S., 2019; Baji, A., 2020; Karabulut, F., 2021; Wu, J., 2022; Casasola, R., 2014]. Samples dissolved in solvents in low concentrations were pipetted onto glass slides inside of a fumehood for a quick evaporation test. This would allow rapid fiber solidification and prevent fibers from adhering together due to existence of residual solvent present during the electrospinning process. The most workable solvent systems for electrospinning PLA were mixtures of DCM: DMF and DCM:DMAc, repectively. Solvent mixtures of DCM:Acetone and Chloroform:THF were found unsuitable for this process [Shao, W., 2023; Zhao, Y., 2024; Wang, L., 2022; Liang, C., 2023; Selatile, M., 2020; Khatsee, S., 2018; Wang, S., 2019; Baji, A., 2020; Karabulut, F., 2021; Wu, J., 2022; Casasola, R., 2014]. DCM:Acetone solvent mixture could clog syringe needles due to fast acetone evaporation, causing frequent stops during electrospinning. The main concern on the use of chloroform and THF was their potential environmental and toxicity concerns, since THF is known to be a female reproductive carcinogen. The ES#1 electrospinning setup was employed in these solvent exploratory tests. Two different solvent solutions were finally tested for producing PLA fibrous membranes, including DCM:DMF (4:1 v/v) and DCM:DMAc (4:1 v/v). Both DMF and DMAc are polar solvents that help the solution to be drawn from the charged needles to the grounded collection device. These solvents have been used previously to successfully electrospin PLA [Shao, W., 2023; Zhao, Y., 2024; Wang, L., 2022; Liang, C., 2023; Selatile, M., 2020; Khatsee, S., 2018; Wang, S., 2019; Baji, A., 2020; Karabulut, F.,

2021; Wu, J., 2022; Casasola, R., 2014; Lo, J., 2022]. SEM images were taken of the materials to further examine the fiber structure and the fiber size in the membranes (Figure 2.2). Additionally, VK3 was added into the PLA solution samples, and the mixtures were successfully electrospun fibrous membranes containing VK3. As seen in Figure 2.2e, the fibers created by the 10% PLA in DCM:DMAc solution produced fibers in varied fiber sizes. Even though both PLA solutions could successfully produce fibrous membranes, the DCM:DMAc system caused more frequent clogs of the needles than the DCM:DMF system. The 4:1 DCM:DMF solvent system resulted in smoother electrospinning operations, and thus was chosen for use in the following research.

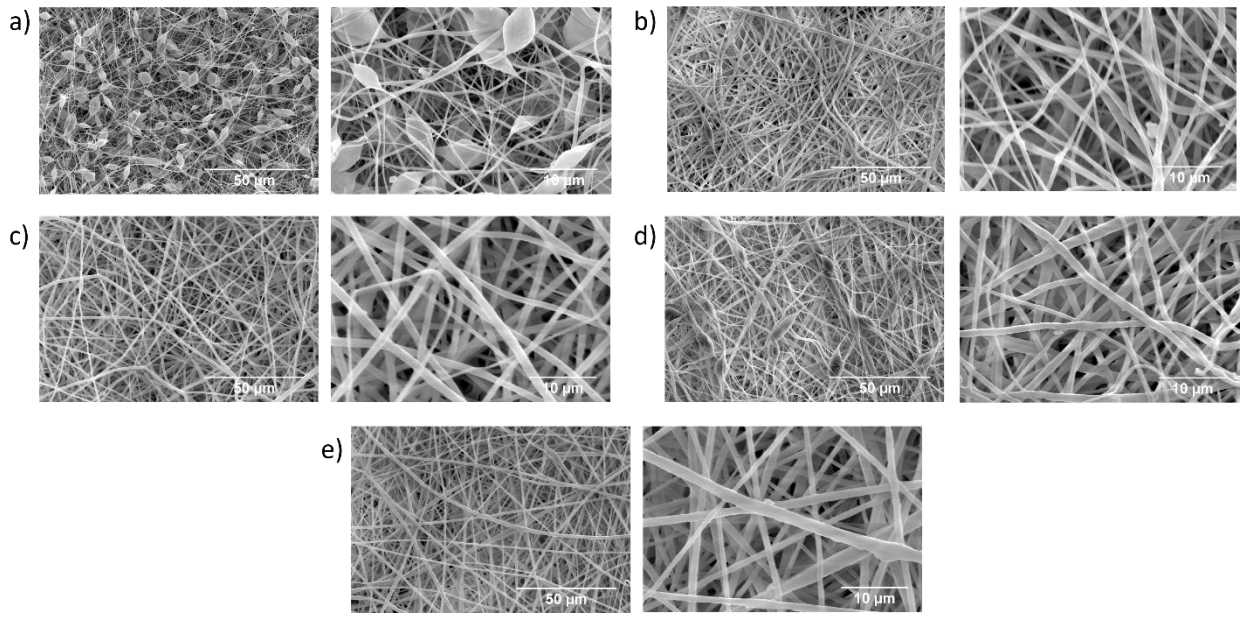

Figure 2.2. SEM images of electrospun PLA membranes using different solvent systems, different concentrations of PLA, and VK3 added (a) membrane electrospun from 8% PLA in 4:1 DCM:DMF solution [Sample A] (b) membrane made from 10% PLA and 8:2 DCM:DMF electrospinning solution [Sample B] (c) membrane made from 12% PLA dissolved in 8:2 DCM:DMF solution [Sample C] (d) membrane made from 10% PLA, 10% VK3 dissolved in 8:2 DCM:DMF solution [Sample D] (e) membrane electrospun from 10% PLA in 8:2 DCM: DMAc [Sample E]

The water contact angles of the electrospun samples were also measured to determine the hydrophilicity of the membranes (Figure 2.3). The hydrophilicity of the fibrous membranes changed little under these varied electrospinning conditions with their contact angles greater than 90°.

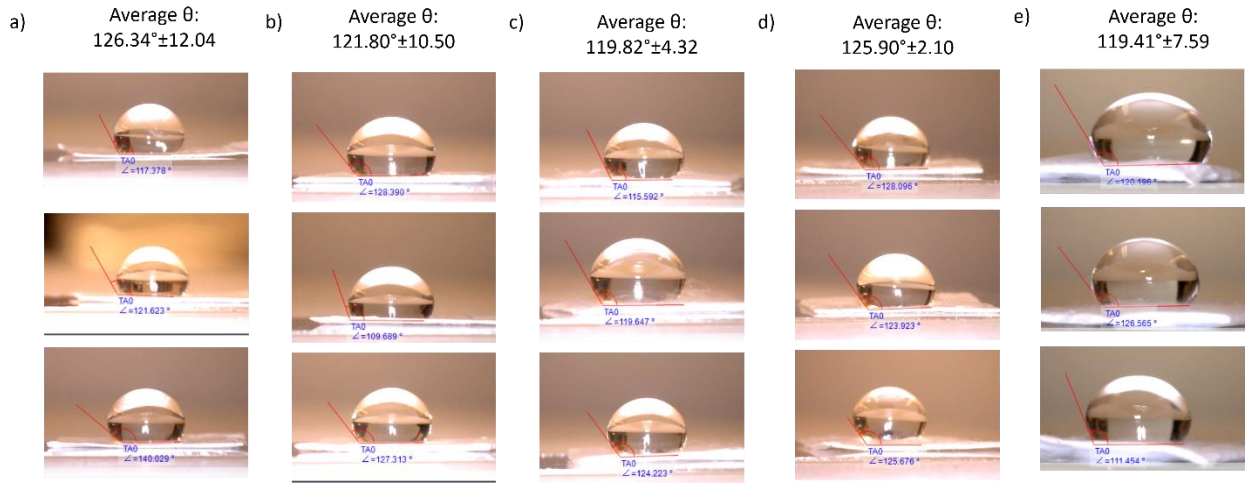

Figure 2.3. Water contact angles of assorted PLA membranes (a) Sample A (b) Sample B (c) Sample C (d) Sample D (e) Sample E

2.4.2 Properties of PLA Membranes

The properties of the electrospun materials were further studied using different PLA solution concentrations and different membrane thicknesses. The following samples were all electrospun using ES#3, which provided better control in the spinning process. The targeted amounts of PLA membranes dispensed onto the collecting device are based on estimations of extrusion speed of the needle pump and a 70% collection efficiency of the polymer onto the collection device. The targeted surface densities of the electrospun membranes were set at 10 g/m^2, 20 g/m^2, 30 g/m^2. Even though 8wt% PLA in solution was shown to create bulbs on the fibers, as seen in Figure 2.2a, the 8wt% PLA solution was explored to see if the bulbs led to a difference in the filtration efficiency and pressure drop across the membrane. Figure 2.4 shows the SEM images of the fibrous membranes and their respective fiber diameter distributions made from solutions in different concentrations of PLA and VK3. The materials are identified by the concentration of PLA in solution (8wt% PLA→S8) and the average surface density of the materials (15

g/m^2→D15); a membrane electrospun with a 8wt% PLA solution in DCM:DMF with an average surface density of 16.03±2.22 g/m^2 is identified as S8D16. The concentrations of PLA in solution explored were 8% PLA, 10% PLA, and 12% PLA based on previous PLA electrospinning research [Shao, W., 2023; Zhao, Y., 2024; Wang, L., 2022; Liang, C., 2023; Selatile, M., 2020; Khatsee, S., 2018; Wang, S., 2019; Baji, A., 2020; Karabulut, F., 2021; Wu, J., 2022; Casasola, R., 2014]. 8 wt% PLA in the DCM: DMF solution created bulbs of polymer on the fibers making the structure inconsistent as seen in Figure 2.4a-c. Figure 2.4d-f display membranes made with 10 wt% PLA in the DCM:DMF and show more even fiber size distribution with minimal bulbs of polymers. Figure 2.4g-i shows SEM images and fiber size distributions of membranes electrospun from using 12% PLA solution, which have a larger variance in fiber diameters than the membranes made from 10% PLA solutions. This data provided a better understanding of the structure of the fibrous membranes as well as the best concentration of PLA for use in future experiments. Figure 2.4j shows the SEM images and fiber size distribution of a membrane containing menadione (VK3), which were electrospun from a 10 wt% PLA and 5wt% VK3 in DCM:DMF solution. These samples demonstrated that the addition of VK3 did not alter the structure of the fibers. These samples also showed similar properties between the those made from using different concentrations of PLA to those earlier samples that were electrospun using the device ES#1. The bulbs of PLA could be observed on both samples spun using 8wt% PLA seen in Figure 2.2a and Figure 2.4a-c. The bulbs of PLA are larger for the samples electrospun using ES#1 in comparison to the samples electrospun using ES#3, which is attributed to the slower speed of the collection device (ES#1).

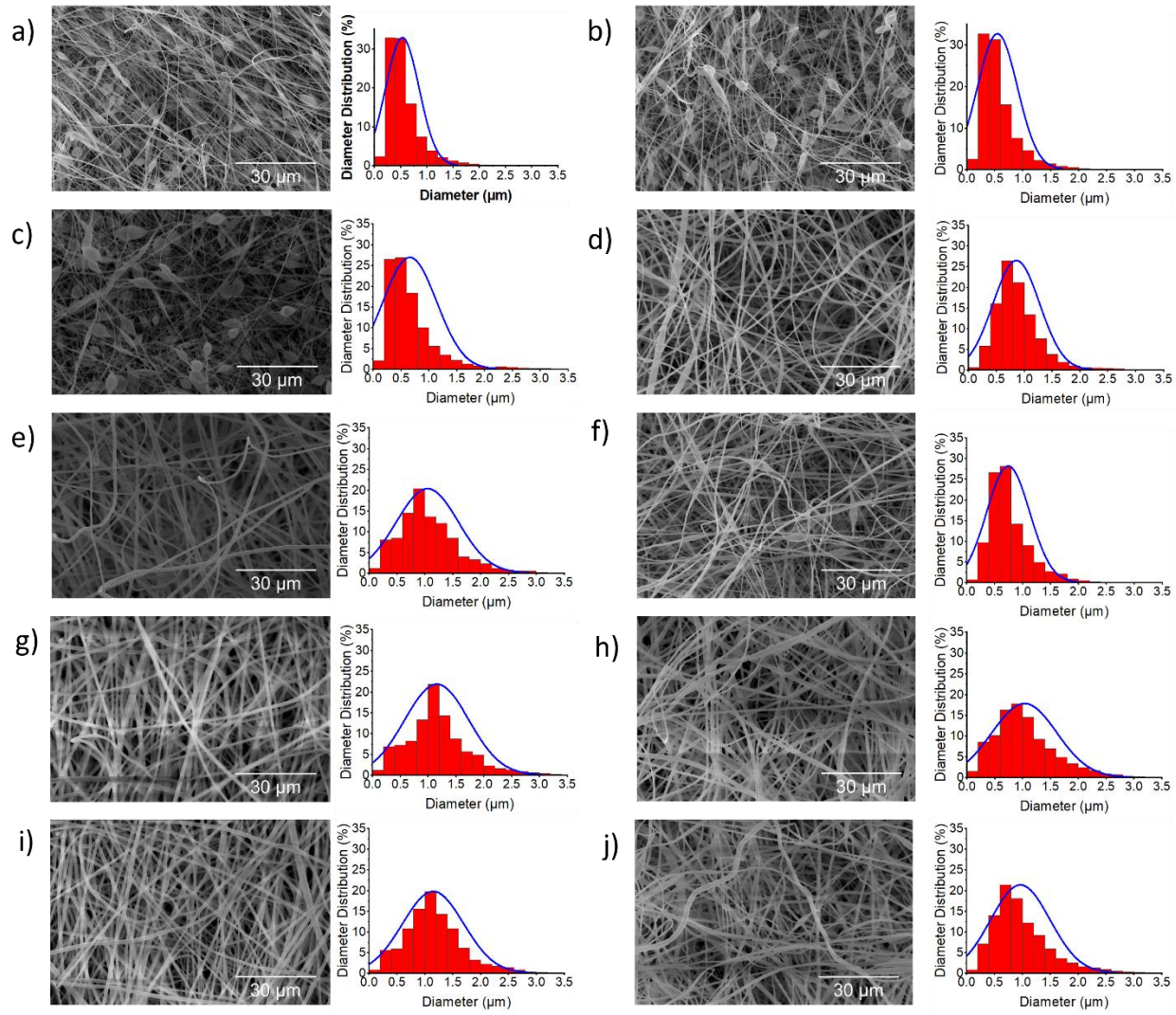

Figure 2.4. SEM images and fiber diameter distributions of different electrospun PLA membranes (a) S8D2 (b) S8D16 (c) S8D19 (d) S10D5 (e) S10D16 (f) S10D23 (g) S12D6 (h) S12D15 (i) S12D26 (j) S10D15-5%VK3

In addition, the water contact angles of these membrane samples were measured (Table 2.1). After statistical analysis of the water contact angles of the materials, the p-value was determined to be 0.229, meaning that the different electrospinning conditions did not statistically impact the water contact angle. This is because the material composition itself is still 100% PLA. The materials containing VK3 are hydrophobic, which can play a role in the attachment of materials to the surface of the fibers as well as the attraction to hydrophilic bacterial cells.

Table 2.1. Material properties of various PLA membranes electrospun with varying concentrations of PLA in solutions.

Sample Name	PLA concentration in solution (%)	Surface Density (g/m^2)	Mean Diameter (µm)	Mode Diameter (µm)	Percent Porosity (%)	Water Contact Angle
S8D2	8	1.89±1.02	0.79±0.18	0.54	52	116.00°±3.00
S8D16	8	16.03±2.12	0.78±0.18	0.54	52	116.73°±0.93
S8D19	8	18.79±10.78	0.88±0.23	0.54	48	136.17°±33.36
S10D5	10	4.86±2.97	1.51±0.32	1.22	44	111.50°±7.45
S10D16	10	16.16±5.55	1.76±0.48	1.76	49	109.13°±4.60
S10D23	10	22.55±6.72	1.18±0.25	1.22	55	115.30°±3.80
S12D6	12	6.17±2.35	2.04±0.50	2.30	48	120.03°±4.97
S12D15	12	14.87±3.14	1.59±0.48	1.76	41	114.60°±3.98
S12D26	12	25.81±4.06	2.12±0.46	2.16	32	111.10°±6.22

Table 2.1 displays the material properties of the samples including the average fiber diameter and the percent porosity of the membrane. For each concentration of PLA in solution, the fiber diameters in resulted membranes in varied thickness stay consistent, while the increase in the PLA concentration in electrospinning solutions lead to increase in fiber diameters. The increased PLA concentration will cause higher viscosity of the electrospinning solution, resulting in a larger fiber diameter. Even though different concentrations of PLA were used, the percent porosity of the membranes does not change significantly.

Breathable filtration materials employed in facemasks should provide high filtration efficiency and low resistance to airflow (low pressure drop). Filtration efficiency and pressure drop tests were employed to evaluate the PLA fibrous membranes produced by the electrospinning process (Figure 2.5a-b). All the membrane materials except for S10D5 display a very high collection efficiency of >90% under flow rates of 30 L/min and 85 L/min, making them good candidates for particle collection. The NIOSH regulation threshold value for pressure drop of facemask filtering materials is <35 mm w.g. for inhalation at a continuous flow rate of 85 L/min [Andrews, R., 2020]. According to this standard, samples of S8D2,

S10D5, S12D6, S12D15, and S12D26 are breathable enough to be used as mask filtration materials. The differences in pressure drop and filtration efficiency readings can be correlated to the average fiber diameter. The samples electrospun from the 12wt% PLA in solution have the largest average diameter as well as the most consistent low pressure drop readings across multiple thicknesses. The results are quite interesting as the S8D2 has finest fiber size and thinnest thickness, while membranes of all S12 samples have coarse fiber sizes. The measured porosity of the membranes slightly decreased from 48-52% to 32-48% (Table 2.1). In fact, fiber diameter of materials affects pore sizes in the system (3D) because finer fibers can pack more closely. When the fiber size is coarse is enough, such as S12 samples, the pore size is big enough and the thicknesses of the samples becomes less important. Thus, PLA fibrous membranes electrospun from 12wt% PLA in solution showed good filtration efficiency (<90%) and a lower pressure drop, making them more breathable to the user. Overall, the best candidates for filtration membranes based on the measured collection efficiency and pressure drop are S10D5, S12D6, and S12D15.

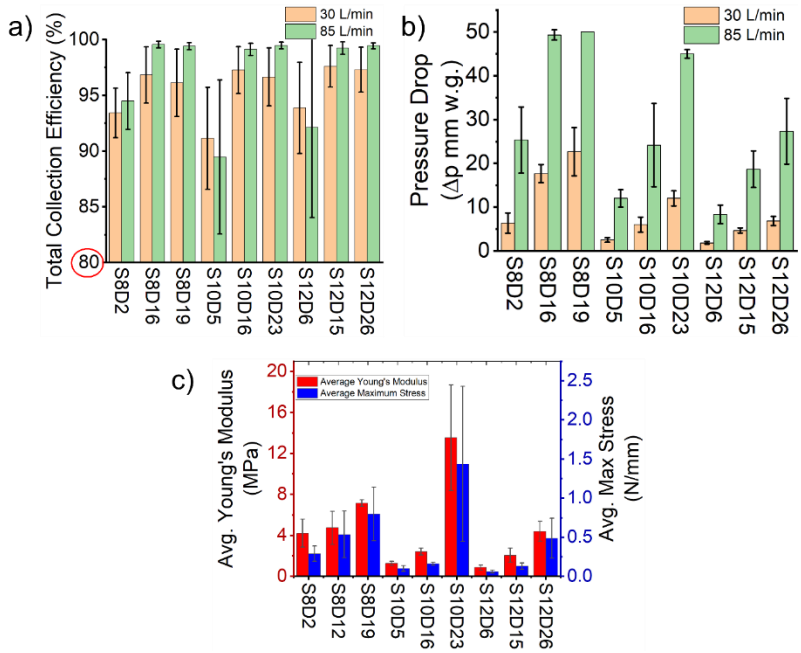

Figure 2.5. Physical properties of various electrospun PLA membranes (a) total collection efficiency (b) pressure drop (c) tensile data in the form of average Young's Modulus and average maximum stress

2.4.4 PLASMA Treatment

Plasma treatment can create hydrophilic groups on the surface of hydrophobic materials [Sheng, L., 2020], which is a common industrial practice nowadays. By simply treating the PLA-VK3 fibrous membrane samples with the plasma cleaner, the materials could become hydrophilic (Figure 2.6a). Hydrophilic surfaces could be wet and in good contact with microbial cells, enhancing antimicrobial functions of the materials. However, since VK3 added into PLA could be attacked by the plasma beams and become damaged, especially if it is present on the surface of fibers. Unfortunately, after the plasma treatment the samples no longer presented the ability to produce $^1O_2$, meaning that the surface bound VK3 might be damaged or fully removed (Figure 2.6b). This method for increasing the hydrophilicity was not used in any further studies due to its reduction of the added agents on surfaces.

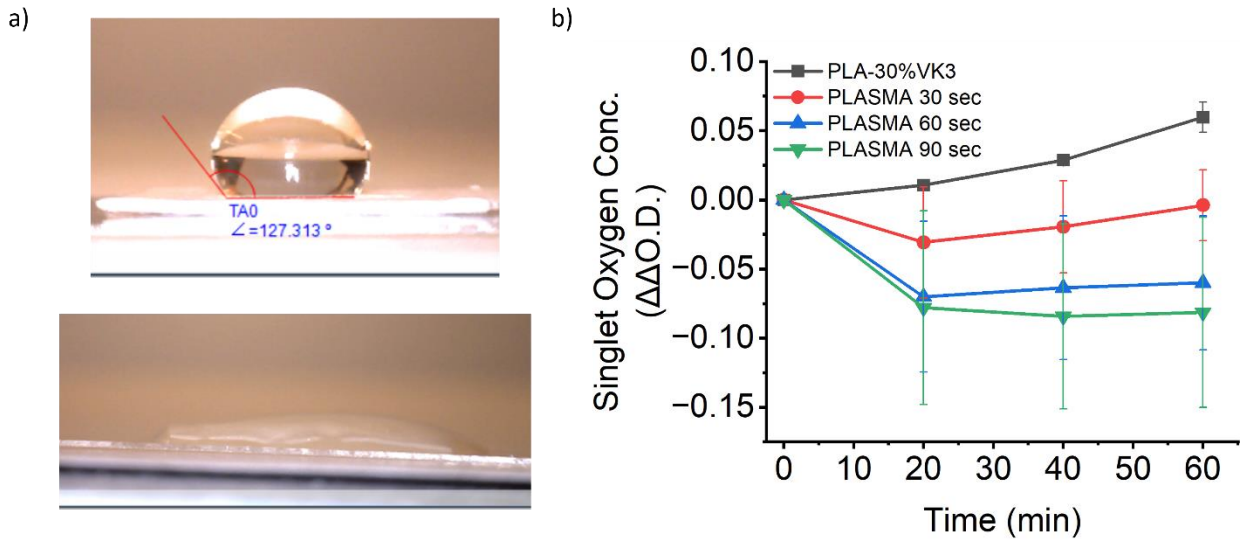

Figure 2.6. PLASMA treatment of PLA-VK3 nanofibrous membranes (a) water contact angle of untreated (top) and 60 seconds PLASMA treated (bottom) PLA-30%VK3 (b) production of singlet oxygen under D65 lighting

2.5 Conclusion

Biodegradable PLA fibrous membranes were fabricated by using an electrospinning process, which could be tested as an alternative to current mask materials. Multiple solvent systems and

electrospinning conditions were explored to produce the PLA membranes, and solvent systems of DCM:DMF and DCM:DMAc were successfully identified and utilized in the study. Additionally, with intension to produce antibacterial and biodegradable filtration materials for facemask uses, an edible photosensitizer, vitamin K3 (VK3) was added into the PLA electrospinning solutions. PLA fibrous membranes containing VK3 (PLA-VK3) were successfully prepared using the same protocol developed from the pure PLA membrane production process. Morphologies and filtration performance of the PLA fibrous membranes were evaluated. Membranes made from 8%-12% PLA solutions were in good morphology and porosity, with lower concentrations resulting in finer fibers. Based on the filtration efficiency and pressure drop data, PLA fibrous membranes made from PLA solutions in 12% concentrations performed better. Even though the PLA membranes are hydrophobic, they still display adequate particle collection efficiency and low pressure drop, in comparison to filtering materials used in facemasks. This study laid foundations for the advanced research activities of my project, which is presented in next chapter.

2.6 References

Andrews, R., Fey O'Connor, P., NIOSH Manual of Analytical Methods (NMAM), Fifth Edition. *Centers for Disease Control and Prevention* (2020).

Baji, A., Agarwal, K., and Oopath, S.V., Emerging Developments in the Use of Electrospun Fibers and Membranes for Protective Clothing Applications, *Polymers*, (2020), 12(2)

Casasola, R., Thomas, N., Trybala, A., et al., Electrospun Poly Lactic Acid (PLA) Fibres: Effect of Different Solvent Systems on Fibre Morphology and Diameter. *Polymer* (2014), 4728-4737, 55(18)

Deng, Y., Si, Y., Sun, G., 33 Fibrous Materials for Antimicrobial Applications. Handbook of Fibrous Materials, 2 Volumes: Volume 1: Production and Characterization/Volume 2: Applications in Energy, Environmental Science and Healthcare. *John Wiley & Sons*, (2020), 927-951

Herman, J., Neal, S., Efficiency comparison of the imidazole plus RNO method for singlet oxygen detection in biorelevant solvents. *Analytical and Bioanalytical Chemistry*, (2019), 5287-5296, 411(20)

Islam, S., Zhang, Z., Zhao, C., Wisuthiphaet, N., Nitin, N., and Sun, G., Design and Development of Robust, Daylight-Activated, and Rechargeable Biocidal Polymeric Films as Promising Active Food Packaging Materials, *ACS Applied Bio Materials*, (2023), 2459-2467, 6(6)

Karabulut, F., Höfler, G., Chand, N., et al., Electrospun nanofibre filtration media to protect against biological or nonbiological airborne particles. *Polymers*, (2021), 13(19)

Kraijic, I., El Mohsni, S., A new method for the detection of singlet oxygen in aqueous solutions. *Photochemistry and Photobiology* (1978), Vol. 28, pp. 577-581

Lawal, U., Robert, V., Loganathan, S., et al., Poly(lactic acid)/Menadione Based Composite for Active Food Packaging Application. *Journal of Polymers and the Environment*, (2023), 1938-1954, 31(5)

Li, G., Zhao, M., Xu, F., et al., Synthesis and Biological Application of Polylactic Acid, *Molecules*, (2020), 25(21)

Liang, C., Li, J., Chen, Y., et al., Self-Charging, Breathable, and Antibacterial Poly(lactic acid) Nanofibrous Air Filters by Surface Engineering of Ultrasmall Electroactive Nanohybrids. *ACS Applied Materials and Interfaces*, (2023), 15, 57636-57648

Lim, L., Auras, R., Rubino, M., Processing technologies for poly(lactic acid). *Progress in Polymer Science (Oxford)*. (2008), 820-852, 33(8)

Lo, J., Daoud, W., Tso, C., et al., Optimization of polylactic acid-based medical textiles via electrospinning for healthcare apparel and personal protective equipment. *Sustainable Chemistry and Pharmacy*, (2022), 30

Khatsee, S., Daranarong, D., Punyodom, W., et al., Electrospinning polymer blend of PLA and PBAT: Electrospinnability–solubility map and effect of polymer solution parameters toward application as antibiotic-carrier mats. *Journal of Applied Polymer Science*. (2018), 135(28)

Maragkaki, A., Malliaros, N., Sampathianakis, I., et al., Evaluation of Biodegradability of Polylactic Acid and Compostable Bags from Food Waste under Industrial Composting. *Sustainability (Switzerland)*, (2023), 15(22)

Mozetič, M., Plasma-stimulated super-hydrophilic surface finish of polymers. *Polymers*. (2020), 1-15, 12(11)

Selatile, M., Ojijo, V., Sadiku, R., et al., Development of bacterial-resistant electrospun polylactide membrane for air filtration application: Effects of reduction methods and their loadings. *Polymer Degradation and Stability*, (2020), 178

Shao, W., Niu, J., Han, R., et al., Electrospun Multiscale Poly(lactic acid) Nanofiber Membranes with a Synergistic Antibacterial Effect for Air-Filtration Applications. *ACS Applied Polymer Materials*, (2023), 9632-9641, 5(11)

Sheng, L., Zhang, Z., Sun, G., Light-driven antimicrobial activities of vitamin K3 against Listeria monocytogenes, Escherichia coli O157:H7 and Salmonella Enteritidis. *Food Control*. (2020), 114

Singhvi, M., Zinjarde, S., Gokhale, D., Polylactic acid: synthesis and biomedical applications. *Journal of Applied Microbiology*, (2019), 1612-1626, 127(6)

Tang, P., Zhang, Z., El-Moghazy, A., et al., Daylight-Induced Antibacterial and Antiviral Cotton Cloth for Offensive Personal Protection. *ACS Applied Materials and Interfaces*, (2020), 49442-49451, 12(44)

Wang, L., Xiong, J, et al., Biodegradable and high-performance multiscale structured nanofiber membrane as mask filter media via poly(lactic acid) electrospinning. *Journal of Colloid and Interface Science*. (2022), 961-970

Wang, S., Liang, J., Yao, Y., et al., Electrospinning-derived PLA/Shellac/PLA sandwich-Structural membrane sensor for detection of alcoholic vapors with a low molecular weight. *Applied Sciences (Switzerland)*, (2019), 9(24)

Wu, J., Liu, S., Zhang, M., et al., Coaxial electrospinning preparation and antibacterial property of polylactic acid/tea polyphenol nanofiber membrane. *Journal of Industrial Textiles*, (2022), 152808372110542

Zhang, Z., Si, Y., Sun, G., Photoactivities of Vitamin K Derivatives and Potential Applications as Daylight-Activated Antimicrobial Agents. *ACS Sustainable Chemistry and Engineering*. (2019), 18493-18504, 7(22)

Zhang, Z., El-Moghazy, A.Y., Wisuthiphaet, N., et al., Daylight-induced antibacterial and antiviral nanofibrous membranes containing Vitamin K derivatives for personal protective equipment. *ACS Applied Materials and Interfaces*, (2020), 49416-49430, 12

Zhang, Z., Wisuthiphaet, N., Nitin, N., et al., Photoactive Water-Soluble Vitamin K: A Novel Amphiphilic Photoinduced Antibacterial Agent. *ACS Sustainable Chemistry and Engineering*. (2021), 8280 8294, 9(24)

Zhao, Y., Ming, J., Cai, S., et al., One-step fabrication of polylactic acid (PLA) nanofibrous membranes with spider-web-like structure for high-efficiency PM0.3 capture. *Journal of Hazardous Materials*, (2024), 165

Chapter 3. Photo-active Antibacterial Polylactic Acid Fibrous Membranes for Facemask Applications

Abstract

Aimed at the development of reusable, biodegradable, and biocidal materials for the next generation of facemasks and respirators, an edible photosensitizer (Vitamin K3, VK3) was successfully mixed with polylactic acid (PLA) in solutions and electrospun into fibrous membranes to prove technical feasibility of producing photo-induced antibacterial and biodegradable fibrous materials. The resulted PLA-VK3 fibrous membranes were directly collected or deposited onto a PLA spunbond nonwoven fabric, simulating a filtering nonwoven structure. The morphologies, mechanical, filtration, photo-active, and antimicrobial functions of the fibrous membranes were assessed. The developed materials revealed promising results of desired filtering efficiency against small particles with low pressure drop, efficient generation of Reactive Oxygen Species (ROS), and antibacterial functions under daylight exposure, as well as proper mechanical properties.

3.1 Introduction

Healthcare workers (HCW) have high risk of occupational infections due to the unavoidable exposure of pathogenic diseases in their working environment. Adequate personal protective equipment (PPE) for HCW is necessary at the working sites. However, the statistics indicate that the HCWs are still the profession with highest infection rate, especially for respiratory infections and the most recent pandemic of COVID-19 an aerosol-based virus [Bandyopadhyay, S., 2020; Verbeek, J., 2016; Tian, C., 2022]. PPE, such as face masks and respirators, indeed protects people from ingesting viral particles and droplets that are spread via aerosol, but only serve as filtering barrier to pathogens [Chaaban, O., 2023]. The used facemasks and respirators still have potential to cause cross-contamination due to the existing live pathogens on the surfaces of the used PPE [Delanghe, L., 2021; Yousefimashouf, M., 2023; Bakhit,

M., 2021]. These residual microbial droplets and particles on the surface of the masks can be easily transmitted to the people who are in touch with them, leading to cross-contamination and increased risk of infections [Bandyopadhyay, S., 2020]. In addition, most PPE materials are single use only and made of non-biodegradable olefin-based polymers that become environmental hazards upon disposal [Li, R., 2021]. Therefore, the development of a new generation of PPE materials with antibacterial and biodegradable properties becomes an urgent need to improve both personal and environmental protection in preparation for future pandemics of SARS-CoV-2 or novel viruses.

In recent years, photo-induced antibacterial functions on materials have been demonstrated with the use of safe and edible vitamins [Escudero, A., 2021; Zhang, Z., 2020; Islam, S., 2023; Sheng, L., 2020; Zhang, Z., 2019; Yap, C., 2023; Lawal, U., 2023]. These chemicals, called photosensitizers, can produce Reactive Oxygen Species (ROS), well known biocides that can kill bacteria and viruses effectively under light (daylight) exposure. The photosensitizers can undergo two different paths of photoreactions, Type I and Type II, to generate different dominating ROS [Zhang, Z., 2021b; Escudero, A., 2021; Zhang, Z., 2020; Sheng, L., 2020; Zhang, Z., 2019]. In both types, the photosensitizer is excited from a ground state to a singlet excited state which undergoes intersystem crossing to a triplet state during irradiation [Delanghe, L., 2021; Yousefimashouf, M., 2023]. Then, ROS species are produced by the triplet excited molecule via a hydrogen abstraction from a polymer or a media (Type I) or collision with triplet oxygen ($^3O_2$) in air (Type II). Type I photosensitizers produce hydrogen peroxide (H_2O_2), hydroxyl radicals (OH^-), or superoxide ($O_2^{-\cdot}$) as dominating ROS, whereas Type II photosensitizers produce singlet oxygen ($^1O_2$) dominantly (Figure S3.1, supplementary information).

Polylactic acid (PLA) is a biobased and biodegradable thermoplastic polymer and could be a good alternative to olefin polymers. PLA has previously been used in combination with nanoparticles and other additives to create antimicrobial filtration materials, sensors, and antibiotic-carrier mats [Shao, W., 2023; Zhao, Y., 2024; Wang, L., 2022; Liang, C., 2023; Selatile, M., 2020; Khatsee, S., 2018; Wang, S., 2019]. Due to the intended use as facemask materials, a vitamin K derivative, menadione/Vitamin K3 (VK3), was selected as the photosensitizer additive since it is potentially edible and has shown the

greatest potential as an antibacterial agent due to its effective production of H_2O_2, $^1O_2$, and OH radical in different polymers and under different light sources of D65, UVA, and UVB [Chaaban, O., 2023; Yousefimashouf, M., 2023]. The use of VK3 as antimicrobial agent for sutures and food packaging have been reported recently [Islam, S., 2023; Yap, C., 2023; Lawal, U., 2023]. VK3 has a melting point of 105-107 °C and proper thermal stability, making it processable in a melt extrusion process with thermoplastic polymers [Islam, S., 2023]. In this study, an electrospinning method was employed to produce daylight-induced antibacterial fibrous membranes that can mimic structures and performances of meltblown or spunbond nonwoven fabrics used in facemasks [Baji, A., 2020; Karabulut, F., 2021]. PLA on its own has been successfully electrospun for use as filtration materials for aerosol and viral capture [Shao, W., 2023; Zhao, Y., 2024; Wang, L., 2022; Liang, C., 2023; Selatile, M., 2020]. The successful fabrication of the functional electrospun PLA fibrous membranes could provide guidance for commercial productions of the biocidal and biodegradable facemask materials [Baji, A., 2020; Karabulut, F., 2021].

3.2 Experimental Materials and Methods

3.2.1 Materials

Polylactic acid 6202D (PLA) was produced by NatureWorks (Minneapolis, MN). Dichloromethane (DCM), dimethylformamide (DMF), Triton X100, and menadione (VK3) were purchased from Sigma Aldrich (St. Louis, MO). *P*-Nitroso-*N*, *N*-dimethylaniline (*p*-NDA) was purchased from TCI Co. Ltd. (Tokyo, Japan). Luria–Bertani (LB) broth, LB agar, tryptic soy broth (TSB), and tryptic soy agar (TSA) were purchased from Thermo Fisher Scientific (Waltham, MA, USA). All the chemicals and supplies were used as received without any further purification. The *Escherichia coli (E. coli* O157:H7, ATCC 700728) was employed in antibacterial tests. Phosphate Buffer Solution (PBS) 10X powder was purchased from Thomas Scientific LLC, USA.

3.2.2 Electrospinning Method

An NE-1600 six channel programmable syringe pump (syringepump.com, USA) was loaded with 2 syringes with 18-gauge 1-inch cannula needles filled with PLA solutions. The cylindrical collection device with a length of 20 cm and diameter of 9 cm rotated at 120 rpm to collect fibrous membranes. A layer of PLA spunbond (18g/m^2) was placed on the collecting drum to produce the layered PLA nonwoven fabrics used for filtration efficiency tests. PLA nonwoven membranes used for ROS and bacterial testing were spun directly onto the collection device. The solution injection speed was set at 1.5mL/hr, and the distance from the end of the needle to the collection device was set at 20 cm. A solvent mixture (DCM/DMF=8:2) was used to dissolve PLA in a concentration range of 10-12 wt% [Zhao, Y., 2024; Wang, L., 2022; Liang, C., 2023; Selatile, M., 2020; Wu, J., 2022; Casasola, R., 2014]. For a 10 wt% PLA solution, 10 grams of PLA were added to 90 mL of the solvent, and for a 12% solution, 12 grams of PLA was added to 88 mL of the solvent. The PLA was dissolved in the solution overnight to ensure complete polymer dissolution before electrospinning. The amount of VK3 added to the PLA solution varied from 1% VK3-5% VK3 as a percentage of the solid in solution. VK3 was added in the day of electrospinning to reduce potential oxidation in the solution. After electrospinning, the fibrous membrane samples were dried at 40°C for 4-5 hours to remove any residual solvent.

3.2.3 Material Characterization

Fourier Transfer Infrared Spectrometry (FTIR) was used to determine the chemical composition of the materials (Thermo Scientific-ATR). The water contact angle was determined by dropping a droplet of water onto a 1cm x 1cm sample and measuring its angle by using a Dino-lite microscope (Dino-Lite Digital Microscope, Taiwan,). The water contact angle values were analyzed using an ANOVA test with a $p\text{-value}<0.05$. The fiber size and fiber morphology of the PLA fibrous membranes were examined through a scanning electron microscope (SEM) (Thermo Fisher Quattro S Environmental SEM). To determine the average fiber diameter and fiber size distribution, an ImageJ image processing software was employed with the use of the DiameterJ plug-in. Thermal properties of PLA samples were evaluated by using a

differential scanning calorimeter (DSC-60, Shimadzu) and a thermogravimetric analyzer (TGA-50, Shimadzu). To determine the tensile strength of the material, samples in size of 3.0 cm x 5.0 cm of each material were prepared and tested using an INSTRON 5566 universal tester following ASTM testing method D5034.

3.2.4 Filtration Performance Tests

The filtration properties of layered PLA membranes (electrospun PLA sandwiched between 2 layers of spunbond PLA of 18 g/m^2) with a size of 16 cm × 16 cm were performed on an 8130 automatic filtration tester (TSI Inc., USA). The filtration efficiency of η (%) and pressure drop of ΔP(Pa) was determined using the NaCI aerosols with a particle size of 0.3 to 0.5 μm at an air face velocity of 120 cm/min (flow rate of 30 L/min) and 340 cm/min (85 L/min), respectively.

3.2.5 Reactive Oxygen Species Testing

Two light sources, D65 and UVA, were used to determine ROS production of the materials, respectively. D65 is the most relevant to the conditions found in hospital indoor environments. The luminosity inside a UV-crosslinker (Spectrolinker XL-1500, USA) containing six 15 W D65 standard daylight tubes (TC-F15T8D) was 15000 Lux, measured by a Dr. Meter LX1330B lux meter with 16 cm distance between the bulbs and the samples. For the UVA (365 nm) light exposure tests, a UV-crosslinker (Spectrolinker XL-1000, USA) equipped with 5- 8W UVA light tubes (Spectroline, BLE-8T365, USA) was used. The distance between the bulbs and the samples was set at 12 cm. Only electrospun PLA membranes were evaluated for the generation of ROS under the light exposure conditions.

3.2.5a Singlet Oxygen Testing

The amount of singlet oxygen ($^1O_2$) produced by the samples was measured by using a 2-solution method [Zhang, Z., 2021b; Zhang, Z., 2020; Islam, S., 2023; Sheng, L., 2020; Zhang, Z., 2019; Herman, J., 2019; Kraijic, I., 1978; Tang, P., 2020; Deng, Y., 2020]. Two separate solutions, *p*-NDA (50 µM) with L-histidine (0.01 M) in PBS and *p*-NDA (50 µM) without L-histidine in PBS, were prepared [Yousefimashouf, M., 2023]. The *p*-NDA solution containing L-histidine reacts with both $^1O_2$ and

hydroxyl radicals produced, bleaching the *p*-NDA in the solution [Kraijic, I., 1978]. The *p*-NDA solution without L-histidine is not able to react with $^1O_2$ but with hydroxyl radicals. A 10 mg electrospun fibrous membrane sample was immersed in 10 mL of each solution. The samples were irradiated under either UVA (365nm) or D65 lighting for times between 0 and 60 minutes. The amount of *p*-NDA left in the solution was measured quantitatively with the absorbance at 440 nm with λ_{max} by a UV-vis spectrometer (Evolution 600, ThermoFisher Scientific, USA). To determine the relative singlet oxygen produced by the sample, the difference in concentrations between the solutions with L-Histidine and without L-histidine was determined following equation 1 [Herman, J., 2019; Kraijic, I., 1978].

$$\Delta\Delta O.D. = (H_0 - H_1) - (P_0 - P_1) \quad (1)$$

Where H_0 = initial 50 µM *p*-NDA with L-histidine solution reading

H_1= 50 µM *p*-NDA with L-histidine solution reading after irradiation

P_0= initial 50 µM *p*-NDA solution reading

P_1= 50 µM *p*-NDA solution reading after irradiation

3.2.5b Hydroxyl Radical Testing

To test the production of hydroxyl radical, a p-NDA (40 µM) deionized water solution was used to quench any hydroxyl radicals (▪OH) produced by the materials when exposed to daylight irradiation [Zhang, Z., 2021; Zhang, Z., 2020; Islam, S., 2023; Sheng, L., 2020; Zhang, Z., 2019; Muff, J., 2011; Tang, P., 2020; Deng, Y., 2020]. 10 mg of the electrospun membrane sample was placed in 10 mL of the solution and irradiated for times between 0 and 60 minutes. The amount of residual *p*-NDA in the solution was measured quantitatively; with the absorbance at 440 nm with λ_{max} by using the same UV-vis spectrometer, following Equation 2.

$$OH \cdot (\mu g\ g^{-1}) = 34 \times 10^6 \times \frac{\Delta C \times V}{m} \quad (2)$$

Where ΔC = difference in concentration between the solution before and after irradiation (mol L^{-1})

V = volume of *p*-NDA solution (L)

m = mass of membrane (g)

3.2.7 Bacterial Testing Protocol

Since the PLA samples could not be sterilized, an *E coli* strain (ATCC 700728) with resistance to rifampicin was employed in the tests [Zhang, Z., 2020; Islam, S., 2023; Tang, P., 2020; Ma, Y., 2022; Zhang, Z., 2021a; Ma, Y., 2021]. Rifampicin (50µg/mL) was added to the molten TSA prior to pouring the agar plates. An *E. coli* suspension in LB was created fresh 24 hours before inoculation of the samples. On the day of inoculation, the *E. coli* was rinsed with 10 mL of PBS three times to remove the growth media, and then diluted with PBS to 5 log CFU/mL. Two drops of sterilized Triton X100 were added to the diluted *E. coli* suspension to help the bacteria adhere to the hydrophobic fibrous membrane. 10 µL of the bacterial suspension and 10 µL of sterilized PBS were loaded onto 1.0 x1.0 cm^2 electrospun membrane samples. The samples were then irradiated under D65 light conditions for a duration of 60 minutes. Every 10 minutes, 10 µL of sterilized PBS were applied to the surface of each sample to prevent the evaporation of the liquid from the surface of the material. After the 60 min of contact with the bacterium and the light exposure, the samples were removed from the irradiation chamber and placed into 2 mL of PBS. The samples were vortexed for 1 minute to remove the bacteria from the surface of the samples and to create a bacterial suspension. After the rinsing process, the bacterial suspension was serially diluted and pipetted onto the agar plates. The bacterial samples were then cultured overnight at 37°C. Bacterial reduction rates are reported following the Equation 3 and Equation 4.

$$\text{Bacteria reduction rate} = 100 * \left(\frac{CFU_{VK3,dark} - CFU_i}{CFU_{VK3,dark}}\right) \quad (3)$$

Where $CFU_{VK3,dark}$= *E. coli* CFU concentration on the surface of PLA-VK3 sample under dark conditions for 60 minutes

CFU_i= E. coli CFU concentration on the PLA-VK3 sample after irradiation

$$\text{Bacteria reduction rate} = 100 * \left(\frac{CFU_{PLA,light} - CFU_i}{CFU_{PLA,light}}\right) \quad (4)$$

Where $CFU_{PLA,light}$= *E. coli* CFU concentration on the surface of PLA sample irradiated under D65 light for 60 minutes

CFU_i= *E. coli* CFU concentration on the PLA-VK3 sample after irradiation

3.2.8 Storage and Light Stability

The storage stability of photoactivity of the PLA-VK3 membranes was evaluated by testing the membrane samples stored under ambient oxygen conditions and low oxygen conditions. The low oxygen samples were wrapped in tinfoil and vacuum sealed into bags using a kitchen vacuum sealer (Ivation model VSP180). Other samples, ambient oxygen samples, were wrapped in tin foil and stored under ambient conditions. Both groups of samples were stored under dark under a constant temperature of 72°F and 40% relative humidity. The photoactivity of the stored membranes was tested by measuring the $^1O_2$ production under UVA lighting conditions on a weekly basis.

The light stability of the PLA-VK3 membranes was quantified via continuous exposure of the membrane samples to a light source [Westek AmerTac, USA]. The LED light source of 1000 Lux of daylight light (5000K) was chosen to simulate the lighting conditions of an examination and treatment room of a hospital [Alzubaidi, S., 2012]. The photoactivity of the materials was measured after 0, 4-, 8-, 16-, and 24-hours exposures of the materials. At each time interval, the photoactivity of the materials was tested by measuring the $^1O_2$ production after irradiation for 60 minutes of the D65 lighting conditions. After determining the photoactivity of the materials, the antibacterial properties of the samples before and after 1000 lux light exposure of 4, 8, and 16 hours were compared. The same testing protocol outlined in section 2.5 was employed to verify the antimicrobial performances of the samples.

3.3 Results and Discussion

3.3.1 Fabrication and Morphology of PLA/VK3 Membranes

In this study, PLA and PLA-VK3 were electrospun into fibrous membranes to prove the expected functions. VK3 was predicted to have good solubility in the electrospinning solvents and good compatibility with PLA based on Hansen Solubility Parameters (HSP) theory and the close HSP distances of the chemicals (Table 1) [Aghanouri, A., 2015]. PLA and PLA-VK3 fibrous membranes containing 1wt%-5wt% of VK3 were prepared from PLA solutions (10-12wt%) using a mixed solvent

system (DCM/DMF = 8/2), and their morphologies were characterized by using an electron scanning microscope (SEM). Figure 1 shows SEM images and fiber diameter distributions of the selected PLA membranes prepared in various concentrations of PLA solution with VK3, and SEM images of other PLA and PLA-VK3 membrane samples are displayed in S2 in supporting materials.

Table 3.1. HSP characteristics of related chemicals and relative HSP distances of solvents, VK3 and PLA

Samples	**Molecular Weight (g/mol)**	**Boiling (T_b)/ Melting (T_m) Point (^{0}C)**	$\boldsymbol{\delta_d}$ **(MPa)**	$\boldsymbol{\delta_p}$ **(MPa)**	$\boldsymbol{\delta_h}$ **(MPa)**	**R1 (PLA)**	R2 (DCM)	R3 (DMF)
PLA	-	168 (T_m)	16.1	13.1	4.9	0	6.64	6.92
DCM	84.9	39 (T_b)	17.0	7.3	7.1	6.64	0	7.70
DMF	73.1	153 (T_b)	17.4	13.7	11.3	6.92	7.70	0
VK3	172.2	105-107 (T_m)	20.2	13.3	6.1	8.29	8.83	7.65

$\boldsymbol{\delta_d}$: dispersion forces; $\boldsymbol{\delta_p}$: polar forces; $\boldsymbol{\delta_h}$: hydrogen bond forces; R: HSP distance between two chemicals

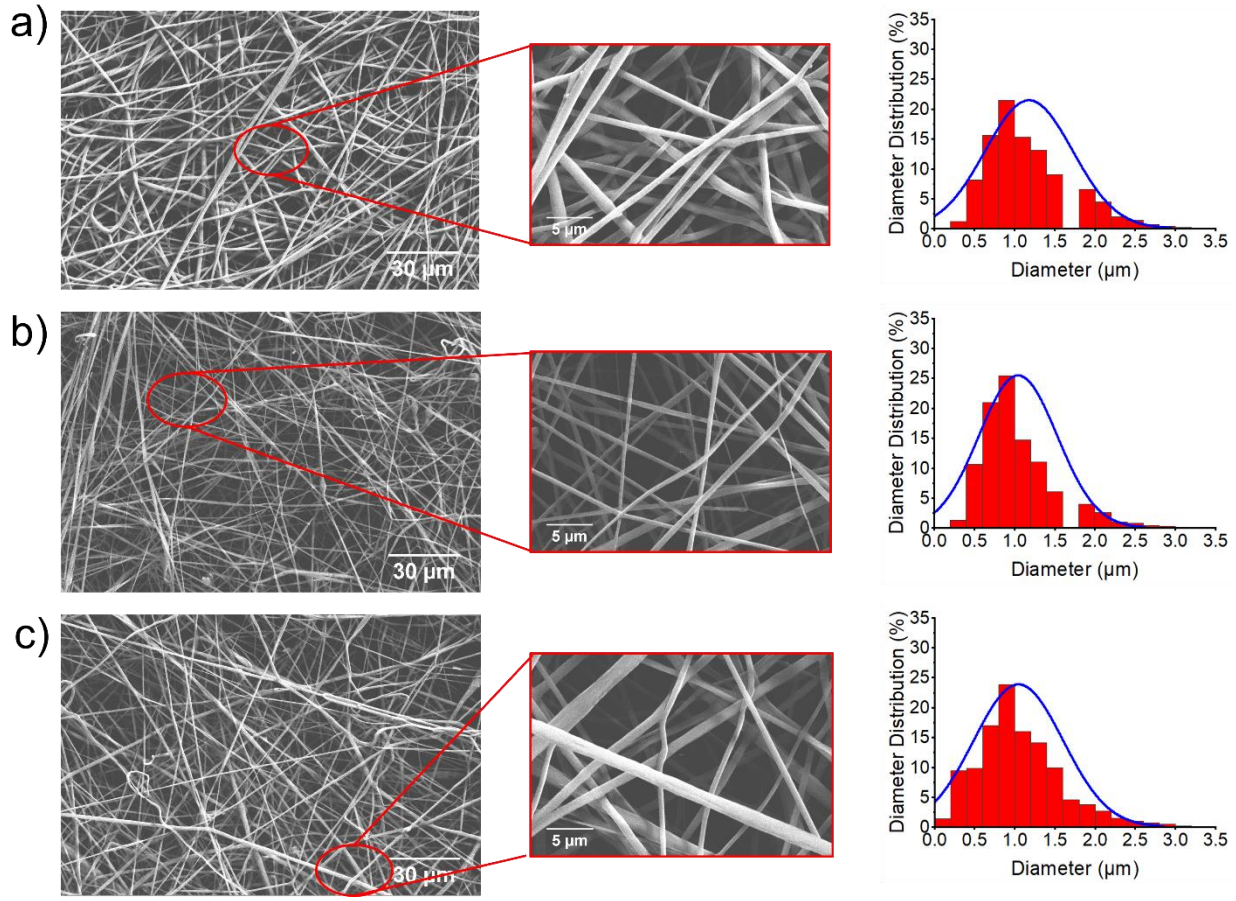

Figure 3.1. SEM images and respective diameter distributions of selected PLA membranes (a) S12D19-1%VK3 membrane electrospun from 12wt% PLA solution with 1wt% VK3 (b) S12D16-3%VK3 membrane electrospun from 12wt% PLA solution with 3wt% VK3 (c) S12D20-5%VK3 electrospun from 12wt% PLA with 5wt% VK3

SEM images of the membranes electrospun from both 12 wt % PLA solutions and 12 wt % PLA-VK3 showed similar morphology, fiber diameters, and their size distributions (Figure 1, Table 2, S2), indicating good compatibility of VK3 with PLA. The average fiber diameters and distributions of the fibrous membranes varied from 1.59±0.48 µm, 2.10±0.28 µm, 1.79±0.08 to 1.92±0.10 µm for membrane samples of S12D15, S12D19-1%VK3, S12D16-3%VK3, S12D20-5%VK3 respectively. With the addition of VK3, the diameters of the fibers in the membranes stay similar and consistent. The porosities of the samples containing VK3 are higher than that of pure PLA samples, which could be correlated to the increased solid content in the solution when VK3 was added, increasing the viscosity of the

electrospinning solution. The addition of VK3 in the range of 1-5wt% in PLA did not cause noticeable changes in surface morphologies of fibers and membranes.

Table 3.2. Material properties of electrospun membranes from solutions containing varied concentrations of PLA and VK3.

Sample Name	PLA Conc. In Solution (%)	Mean Diameter (μm)	Percent Porosity (%)	Surface Density g/m2
S12D15	12	1.59±0.48	41%	14.87±3.14
S12D19-1%VK3	12	2.10±0.28	44%	18.71±2.90
S12D16-3%VK3	12	1.79±0.08	49%	15.48±6.67
S12D20-5%VK3	12	1.92±0.10	47%	19.57±1.28

3.3.2 Characterization and Properties of PLA-VK3 Membranes

The structures of PLA and PLA-VK3 fibrous membranes were characterized by using FTIR analysis. Figure 3.2a confirms the presence (C=O, 1668 cm^{-1}) of VK3 in the PLA-VK3 membrane containing 5 wt% VK3. Thermal properties of the PLA-VK3 membranes were assessed by using both DSC and TGA (Figure 3.2b and 3.2c). The addition of VK3 slightly reduces the glass transition temperature, the cold crystallization, and the melting temperature of the membranes, as shown in DSC spectra in Figure 3.2b. When the VK3 content in the fibrous membrane was increased from 0-5 wt%, the glass transition temperature decreased from 66 °C to 60 °C, a 6°C decrease, while the cold crystallization temperature decreased by 3-6°C, and the melting temperature decreased by 1-3°C. These results are similar to a previous study on PLA-VK3 composite food packaging films [Lawal, U., 2023]. However, the crystallization temperatures (77-83 ^{o}C) of the membranes are much lower than those (97 -126^{o}C) reported for the films. The lower crystallization temperature in the electrospun PLA membranes was noticed in other studies as well, which is mainly caused by immature crystallization and unstable crystal structures formed during the rapid solidification of PLA fibers after the solution electrospinning [Sun, Y., 2024]. Additional heating could remove the unstable elements and stabilize the crystal structure with consistent crystallization temperature of 124^{o}C (Figure 3.2c).

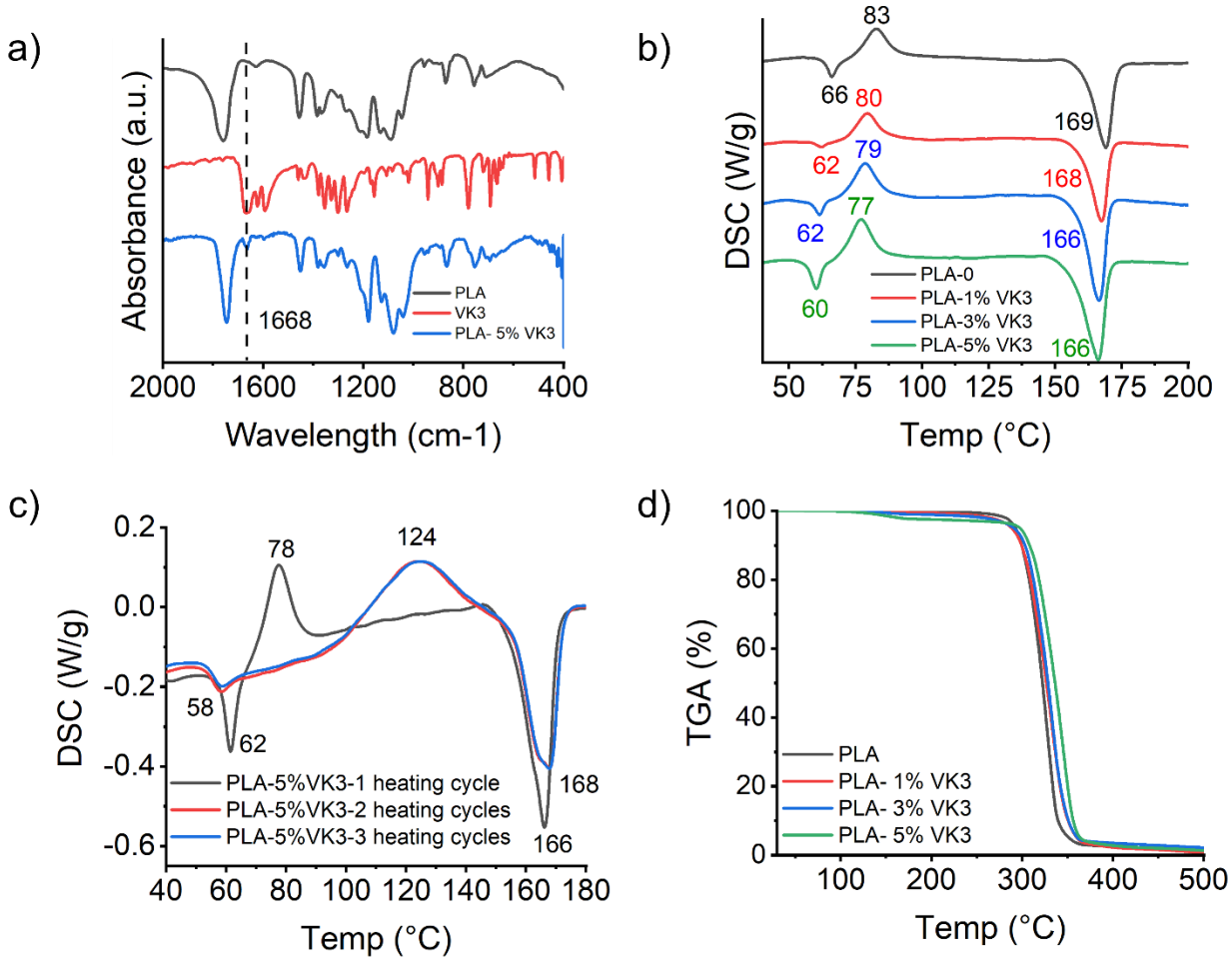

Figure 3.2. Material characterization of electrospun PLA and PLA-VK3 membranes (a) FTIR and (b) DSC analysis of PLA membranes with varied VK3 concentrations (c) DSC spectra of PLA samples after repeated heating (d) TGA analysis of PLA membranes with varied VK3 concentrations.

TGA analysis results of these membranes are shown in Figure 3.2d, and some of key results together with the DSC data are summarized in Table 3. The addition of VK3 did not significantly change the decomposition temperature of the membranes according to an ANOVA analysis the p-value=0.381, which is greater than 0.05, showing no statistical differences between the decomposition temperatures. Weight losses of the membranes at 180°C could provide some clues on whether VK3 could survive heating around this temperature, a possible melt processing condition for the polymer mixtures. Pure PLA exhibited negligible weight loss, whereas the losses of PLA-VK3 increased accordingly with increased VK3 content in the membranes at 180°C, though the lost amounts were still less than that of the added VK3. This means even though VK3 may sublime or degrade under this high temperature, leading to the

weight losses during the heating, there are still enough VK3 present in the material after 1 heating cycle. However, high temperature used in meltblowing process could be a concern for the future use of the PLA-VK3 mixture. Additionally, the weight loss of PLA-VK3 could be mainly the loss of VK3 on surfaces of the fibers during the heating, which brings in concerns of the stability of PLA-VK3 under long term exposure to air as well, since VK3 on the surfaces could interact with oxygen.

Table 3.3. Material characteristics of PLA and PLA-VK3 membranes with various concentrations of VK3.

Samples	Tg	Tc	Tm	Td	% Mass Loss at 180 °C	Water Contact Angle
PLA	66°C	83°C	169°C	358.87±7.21	0.02±0.21	109.93°±4.60
PLA-1% VK3	62°C	80°C	168°C	359.47±1.80	0.31±0.15	111.5°±7.98
PLA-3% VK3	62°C	79°C	166°C	360.60±5.40	0.87±0.13	116.5°±3.32
PLA-5% VK3	60°C	77°C	166°C	355.62±9.24	2.32±0.02	102.43°±16.67

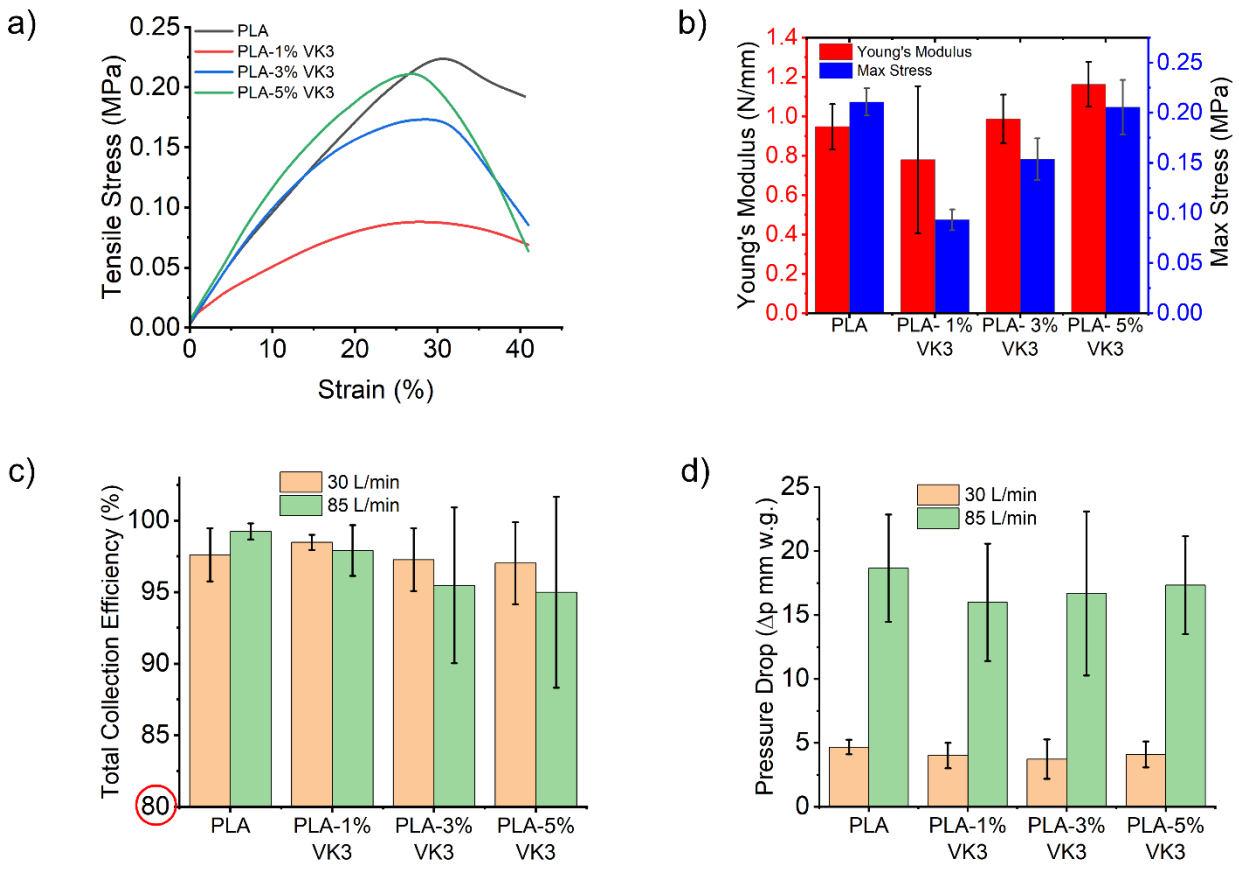

Figure 3.3. Mechanical properties of electrospun PLA and PLA-VK3 membranes (a) stress-strain curves for PLA membranes with varied VK3 concentrations (b) Young's modulus and maximum stress for PLA membranes with varied VK3 concentrations (c) filtration efficiency and (d) pressure drop across PLA membranes with varied VK3 concentrations.

The tensile properties of the PLA and PLA-VK3 membranes were tested, with values of measured Young's Modulus and average maximum stress listed in Table 3.3. The thicknesses and evenness of the electrospun membranes were not fully controllable in a lab-scale device. But the produced membranes did not reveal significant impact of the added VK3 molecules to both Young's modulus and maximum stress values, as well as to their stress-strain curves (Figure 3.3a-b). The varied Young's moduli (from 0.78±0.37, 0.98±0.12, 1.16±0.1 N/mm) and maximum stress values (0.09±0.01, 0.15±0.02, 0.21±0.03 MPa) for PLA-1% VK3, PLA-3% VK3, and PLA-5% VK3, respectively were similar to the properties of pure PLA membranes (Figure 3.3b), except for the PLA-1% VK3 membrane, which could be caused by the unevenness of the membranes. VK3 is a small molecule in solid status in PLA, which may only serve as a filler and could not provide desired plasticizing effect to reduce rigidity of PLA

fibrous membranes. Due to the close HSP distance or good affinity of VK3 to PLA, the fibers formed by the polymeric mixture could retain the PLA features.

Filtration properties of the fibrous membrane materials, including collection efficiency against particles (0.3um) and pressure drop values, are important features to serve as a filtering material within facemasks and respirators. The measured collection efficiencies and pressure drop values of the membranes under two air flowing rates are shown in Figure 3.3c-d. The addition of VK3 in a range of 1-5 wt% in PLA membranes did not significantly affect the filtration efficiency of the materials under both low and high air flow rates. The increase of VK3 content in the material seems to lead to a slight drop in filtration efficiency, but the impact was minimal and the filtration efficiencies were all above 95%. The pressure drop values of the membranes were all far below that the values defined by the NIOSH regulations (42 CFR 84.180), at <35 mm w.g for an inhalation flow rate of 85 L/min [Andrews, R., 2020]. This indicates that the additive VK3 has no impact on the pressure drop of PLA membrane materials, which is another evidence of good compatibility of VK3 to PLA. The PLA-VK3 fibrous membranes are suitable to serve in a N95 respirators.

Since VK3 is water insoluble and hydrophobic, similar to PLA. The addition of VK3 into PLA would not alter the hydrophilicity and hydrophobicity of the membranes (Table 3.3). After a statistical analysis, it was determined that the p-value for the water contact angle was 0.41, which is greater than 0.05, indicating that the water contact angles are not statistically significantly different among the samples with and without the addition of VK3.

3.3.3 Photoactivity of PLA-VK3 Membranes

The addition of VK3, a photosensitizer, in PLA fibers leads to the production of biocidal ROS under light irradiation. The VK3 in PLA could undergo both type I and type II photo reactions, as seen in S1 [Zhang, Z., 2020], forming hydroxyl radicals (type I) or singlet oxygen (type II) as representative ROS, respectively. The relative amounts of singlet oxygen from membranes containing 0%, 1%VK3, 3%VK3 and 5% VK3 under 60 min exposure of D65 or UVA are shown in Figure 3.4a-b. The singlet

oxygen production increases over the course of 60 minutes under both prolonged UVA and D65 exposures. The amounts of hydroxyl radicals of the same membranes under the same exposure conditions and duration are shown in Figure 3.4c-d, and the values were increased accordingly to the increase of VK3 contents in PLA. The increase of VK3 content in PLA resulted in generation of both hydroxyl radicals and singlet oxygen. D65 seems quite weak in degenerating ROS on PLA-VK3 than UVA light as the amounts of both singlet oxygen and hydroxyl radicals. One of the reasons is that the λ_{max} of VK3 is at 333nm (UVA), and another one is that UVA light has better penetrating power than daylight [Fukuoka, H., 2023] . After a comparison with the use of VK3 in other fibrous membranes and films, such as poly(vinyl alcohol-co-ethylene) (PVA-co-PE), polyacrylonitrile (PAN) and poly (ethylene ethyl acetate) (EVA) [Zhang, Z., 2020; Islam, S., 2023], the amounts of generated ROS in PLA were relatively lower than those generated in these polymers in the same concentration of VK3. Hydrophobicity of both PLA and VK3 could affect effective capturing and measurements of produced ROS in aqueous systems, leading to large errors observed in Figure 3.4. In addition, all three other polymers are better hydrogen donors than PLA due to the existence of tertiary C-H in polymer chains. As a result, all of them could produce significant amounts of hydroxyl radicals, product of the type I photo-reaction.

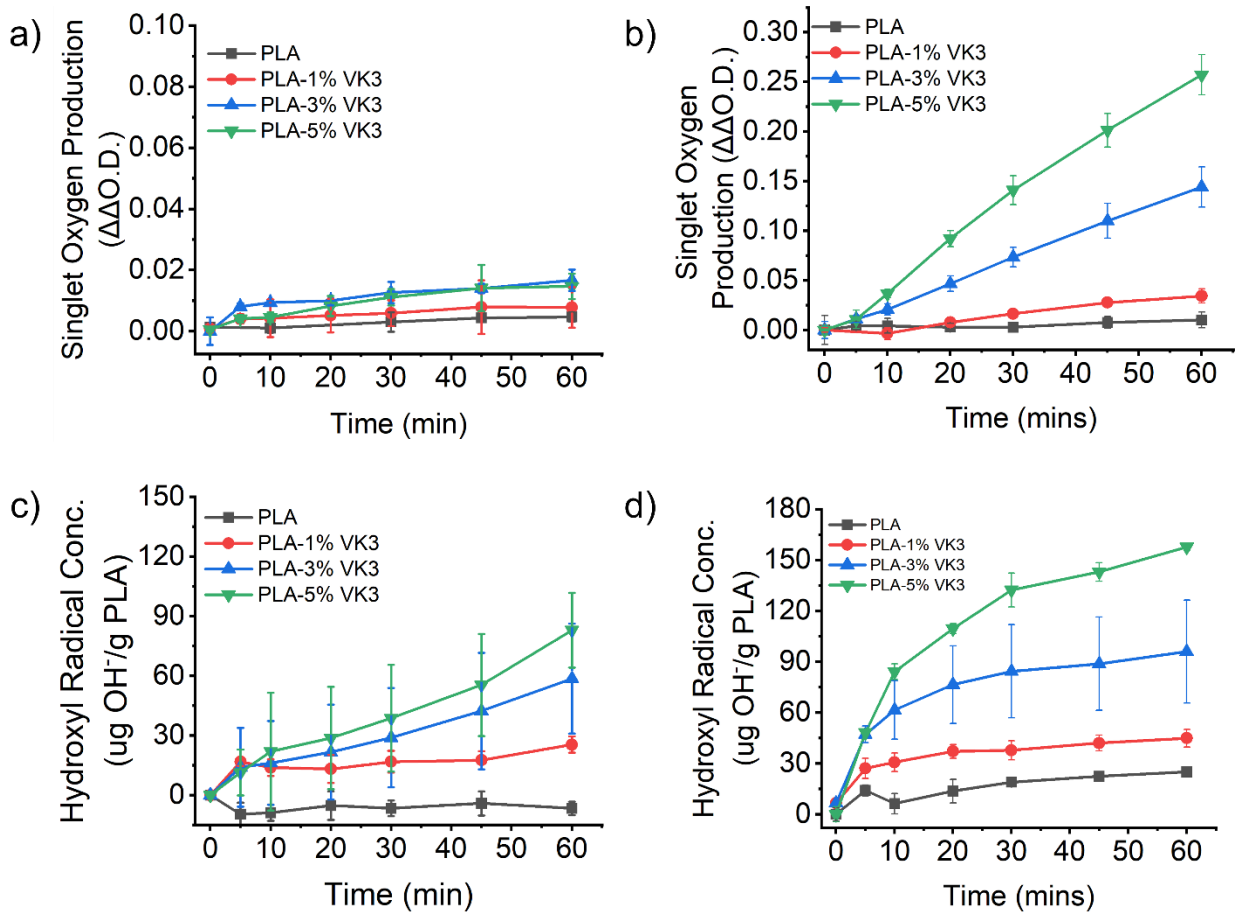

Figure 3.4. ROS production of various PLA and PLA-VK3 membranes (a) $^1O_2$ production under D65 lighting conditions (b) $^1O_2$ production under UVA lighting conditions (c) ▪OH production under D65 lighting conditions (d) ▪OH production under UVA lighting conditions

3.3.4 Stability of PLA-VK3 Membranes

The photoactivity of PLA-VK3 membranes containing different concentrations of VK3 could be affected by oxygen in air or continuous daylight exposure, which impact the storage and continuous use (light exposure) stability of the materials. The oxygen stability of the membranes was examined by storing vacuum sealed PLA-VK3 membranes in both vacuum sealed (low oxygen-LO) and open wrapped PLA-VK3 membranes (ambient oxygen- AO) under ambient conditions in dark. Membrane samples containing 3% VK3 and 5%VK3 were chosen to examine, due to their demonstrated efficacy in production of ROS. The ROS generated by the membrane samples were measured under 60 minutes of

UVA exposure after being stored for up to four weeks. Figure 3.5a shows the photoactivity retention changes measured in the amounts of singlet oxygen production for PLA-3%VK3 and PLA-5%VK3 membranes. Most of the losses of photoactivity occurred in the first week for both concentrations of VK3 stored under LO and AO. Overall, after stored for four weeks, all samples showed significant losses of generated singlet oxygen under the same irradiation conditions. The LO conditions provided by using the food vacuum packaging device was not ideal, which leads to no obvious difference in keeping the photo-reaction of VK3 in PLA versus the AO conditions. However, more VK3 on surfaces of PLA fibers could experience more damage by oxygen or light and may reveal relatively lower retention rates of the photoactivity. As a matter of fact, the photoactivity retention rates measured in production of $^1O_2$ were 42% and 58% for PLA-3%VK3 and 19% and 18% for PLA-5% VK3 under LO conditions and AO conditions, respectively (Figure 3.5a). More VK3 in PLA indeed resulted in more losses of the photoactivity during the storage and light exposure. This leads to the belief that there is the potential for excess VK3 present on the surface of the membranes; meaning that the concentration of VK3 present in the membrane is important. The relative low stability of VK3 in PLA films was also reported in literature [Lawal, U., 2023]. Due to the low production of singlet oxygen over time during the stability test, there is no significant difference between the storage conditions. This experiment reflects the instability of VK3 over time.

The light stability of VK3 in PLA was investigated by exposing the membranes continuously to an LED (daylight) light source to mimic usage in a hospital setting [Alzubaidi, S., 2012]. The samples were placed in a box with the light source providing 1000 lumens on the samples for a duration of up to 16 hours. Then the membrane samples were exposed D65 light for 60 min, amounts of singlet oxygen generated by the membranes were measured, which are shown in Figure 3.5b. The continuous light exposure of VK3 in PLA could quickly consume VK3 molecules on the surfaces of PLA fibers, leading to significant losses of photoactivity of the membranes. The different concentrations of VK3 in PLA did not impact the light stability of the membranes, since the surface bonded VK3 are photoreactive and

vulnerable to light. However, it was found that the hydrophobic PLA membranes could result in difficulty in measuring ROS production in aqueous solution system, leading to relatively large errors in the data. As a result, even though a large amount of surface VK3 were damaged by the LED light, small quantities of $^1O_2$ were produced under D65 lighting exposure after continuous light exposure from 4-16 hours.

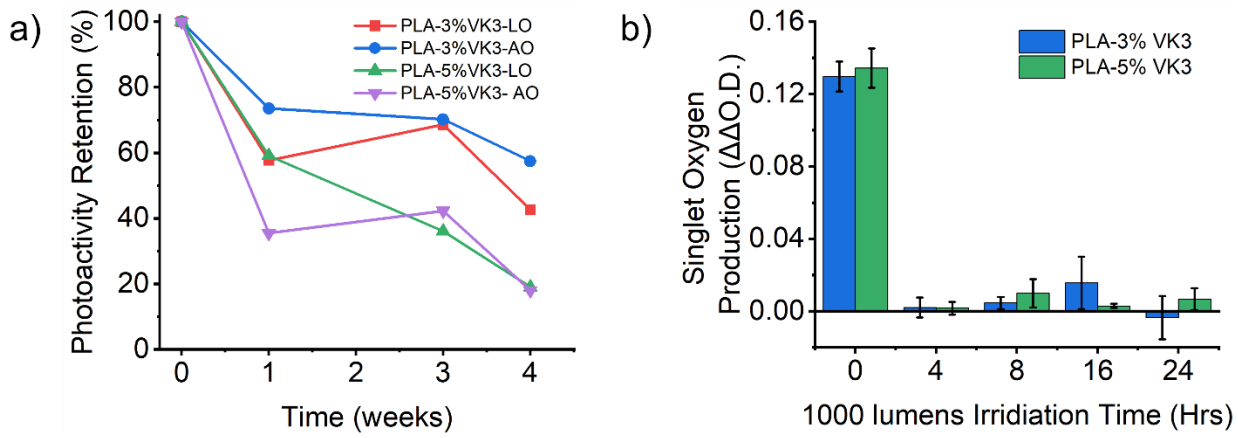

Figure 3.5. Storage tests of PLA-3%VK3 and PLA-5%VK3 samples (a) photoactivity retention of $^1O_2$ over 4 weeks; Light stability tests of PLA-3%VK3 and PLA-5%VK3 samples (b) singlet oxygen production after exposure to 1000 lumens for various time periods

3.3.5 Antibacterial Function

The photo-induced generation of ROS by PLA-VK3 membranes will produce antimicrobial effect on the materials. Antibacterial functions of the PLA-VK3 fibrous membranes were evaluated by testing against a selected *E. coli* strain under D65 light exposure following a method reported in literature [Zhang, Z., 2020; Islam, S., 2023; Tang, P., 2020; Ma, Y., 2022; Zhang, Z., 2021a; Ma, Y., 2021]. Figure 3.6a shows that the increase of VK3 content in the PLA and prolonged exposure time on the membranes lead to increased reduction of the amount of *E. coli* on the surface of the membranes, calculated using Equation 3. A higher concentration of VK3 (3%, 5%) can kill more bacteria under the same light exposure duration compared to a lower concentration of VK3 (1%). The most bacteria reduction occurred between 30 and 60 minutes of the daylight exposure time. The membranes containing 5% VK3 were able to reduce

E. coli concentration by 87% in 60 min of D65 irradiation, while the one containing 3%VK3 reduced about 78% of *E. coli* concentration, indicating that VK3 on surfaces of the fibrous materials performs the functions and a sufficient concentration of VK3 is needed. The hydrophobic nature of PLA and PLA-VK3 also causes slow antibacterial performance because of poor contact of bacteria cells with the fiber surfaces. Thus, prolonged exposure time could increase the antibacterial efficiency due to improved bacteria contact with fiber surfaces. Increase of hydrophilicity of the membranes could improve the antibacterial functions of the membranes, which has become a direction in future studies. Figure 3.6b shows the retention of antibacterial properties of the membrane undergoing prolonged exposure to an LED light source, calculated using Equation 4 (Figure 3.6b-c). Even after 16 hours of extended light exposure, the samples still retained 40% of original antimicrobial power against *E. coli* present on the surface, though the measured singlet oxygen was quite minimal. But the titration measurement of ROS has some errors on hydrophobic surfaces.

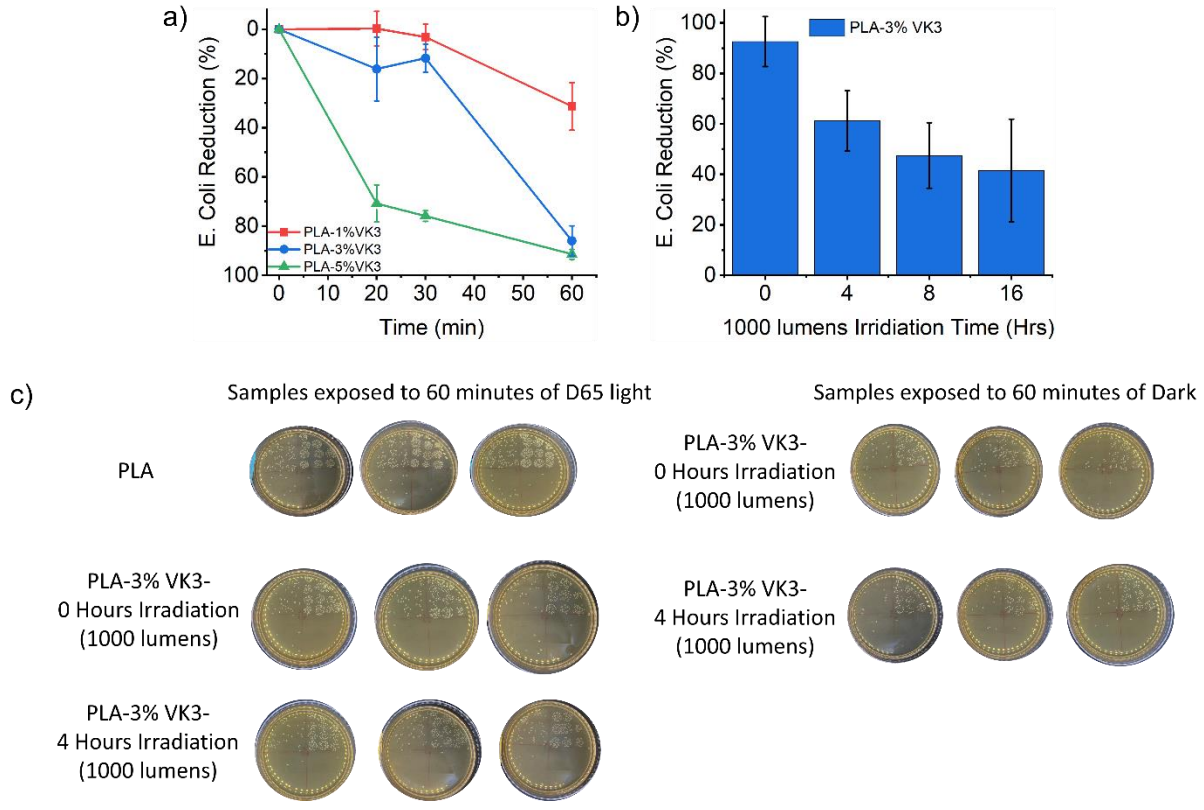

Figure 3.6. *E. Coli* antibacterial tests under D65 lighting conditions (a) bacteria reduction caused by PLA-VK3 samples under D65 light exposure (b) retention of antimicrobial functions of PLA-3%VK3 samples after exposed to

light in relation to the original function under the same conditions (c) plates displaying the bacterial reduction of some samples shown in 6b.

3.4 Conclusion

PLA was successfully electrospun into fibrous membranes using a solvent system, and the membranes possess the desired nonwoven fabric structures. The addition of a Vitamin K derivative, VK3, into PLA polymers did not significantly alter the membrane structure and was able to result in photo-activities on the membrane materials. The PLA-VK3 membranes showed proper filtration efficiency, low pressure drops, and tensile properties, suitable for filtration materials used for facemasks. The demonstrated photoactivities and daylight-induced antibacterial functions of the membranes could improve protective performance of facemasks and protection of people from infections caused by ingesting pathogens. The use of biodegradable PLA in the functional filtration materials could reduce environmental burden caused by the use of PPE. However, the long-term storage stability of PLA-VK3 should be further improved.

3.5 Supplementary Information

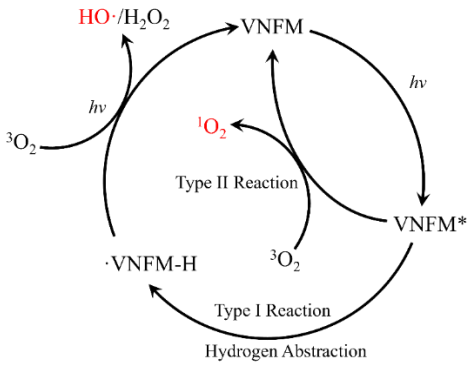

Figure S3.1 Photosensitizer mechanism displaying type I and type II photosensitizers.

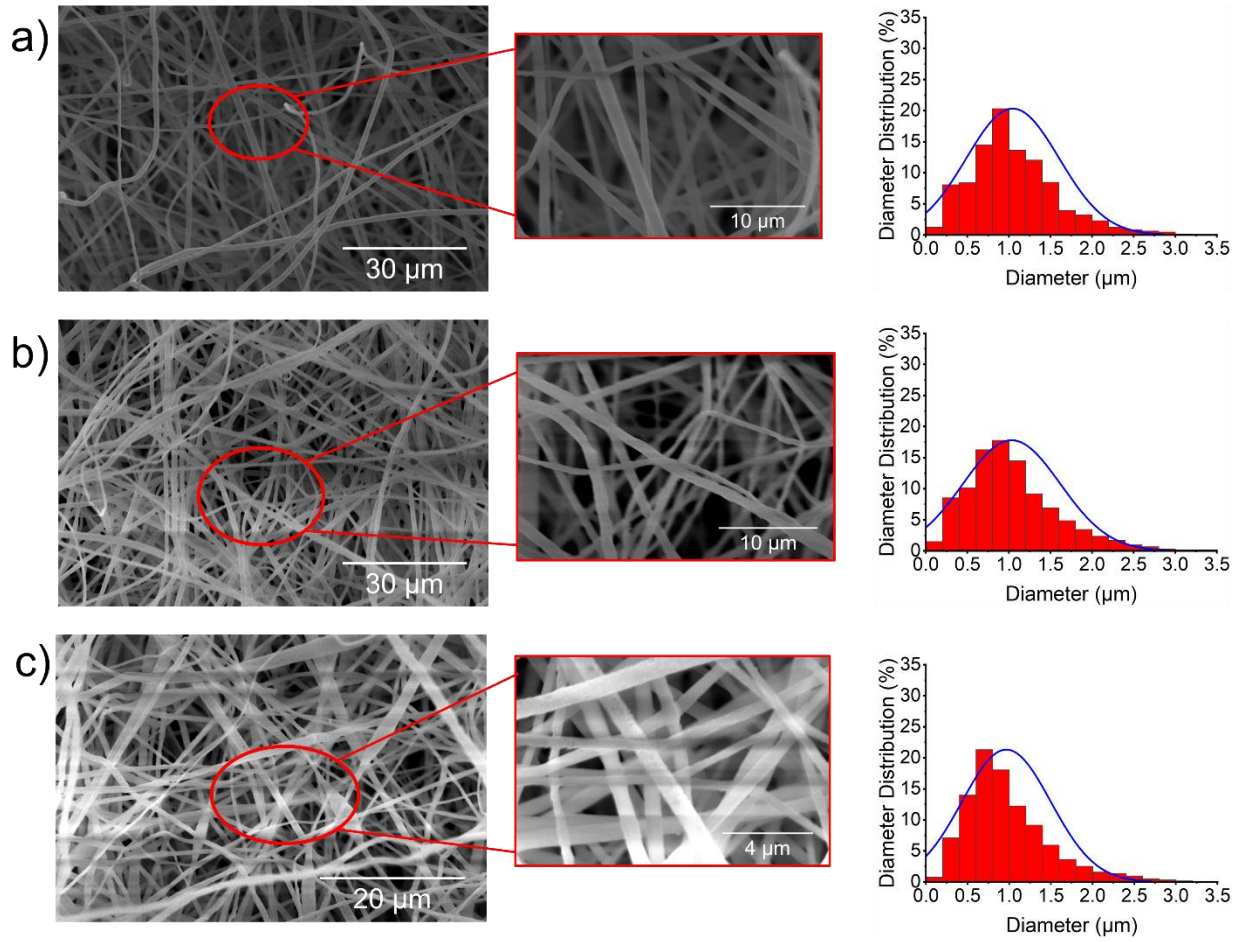

Figure S3.2 SEM images and respective diameter distributions of selected PLA membranes (a) S10D16-membrane electrospun from 10wt% PLA solution (b) S12D15- membrane electrospun from 12wt% PLA solution (c) S10D15-5%VK3 electrospun from 10wt% PLA with 5wt% VK3 based on PLA.

3.6 References

Aghanouri, A., & Sun, G. (2015). Hansen solubility parameters as a useful tool in searching for solvents for soy proteins. *RSC Advances*, *5*(3), 1890–1892

Alzubaidi, S., Soori, P., Energy Efficient Lighting System Design for Hospitals Diagnostic and Treatment Room—A Case Study, *Journal of Light & Visual Environment*, (2012), Volume 36(1), 23-31,

Andrews, R., Fey O'Connor, P., NIOSH Manual of Analytical Methods (NMAM), Fifth Edition. *Centers for Disease Control and Prevention* (2020).

Baji, A., Agarwal, K., and Oopath, S.V., Emerging Developments in the Use of Electrospun Fibers and Membranes for Protective Clothing Applications, *Polymers*, (2020), 12(2)

Bakhit, M., Krzyzaniak, N., Scott, A., et al., Downsides of face masks and possible mitigation strategies: A systematic review and meta-analysis, *BMJ Open*. (2021), 11(2)

Bandyopadhyay, S., Baticulon, R., Kadhum, M., et al., Infection and mortality of healthcare workers worldwide from COVID-19: A systematic review. *BMJ Global Health*, (2020), 5(12)

Casasola, R., Thomas, N., Trybala, A., et al., Electrospun Poly Lactic Acid (PLA) Fibres: Effect of Different Solvent Systems on Fibre Morphology and Diameter. *Polymer* (2014), 4728-4737, 55(18)

Chaaban, O., Balanay, J., Sousan, S., Assessment of best-selling respirators and masks: Do we have acceptable respiratory protection for the next pandemic? *American Journal of Infection Control*, (2023), 388-395, 51(4)

Delanghe, L., Cauwenberghs, E., Spacova, I., et al., Cotton and Surgical Face Masks in Community Settings: Bacterial Contamination and Face Mask Hygiene. *Frontiers in Medicine*. (2021), 8

Deng, Y., Si, Y., Sun, G., 33 Fibrous Materials for Antimicrobial Applications. Handbook of Fibrous Materials, 2 Volumes: Volume 1: Production and Characterization/Volume 2: Applications in Energy, Environmental Science and Healthcare. *John Wiley & Sons*, (2020), 927-951, 2(1)

Escudero, A., Carrillo-Carrion, C., Castillejos, M., et al., Photodynamic therapy: photosensitizers and nanostructures. *Mater. Chem. Front*., (2021), 3788-2812, 5(10)

Fukuoka, H., Gali, H.E., Bu, J.J., Sella, R., Afshari, N.A., Ultraviolet light exposure and its penetrance through the eye in a porcine model. *Int J Ophthalmol*. (2023), 172-177,16(2)

Herman, J., Neal, S., Efficiency comparison of the imidazole plus RNO method for singlet oxygen detection in biorelevant solvents. *Analytical and Bioanalytical Chemistry*, (2019), 5287-5296, 411(20)

Islam, S., Zhang, Z., Zhao, C., Wisuthiphaet, N., Nitin, N., and Sun, G., Design and Development of Robust, Daylight-Activated, and Rechargeable Biocidal Polymeric Films as Promising Active Food Packaging Materials, *ACS Applied Bio Materials*, (2023), 2459-2467, 6(6)

Karabulut, F., Höfler, G., Chand, N., et al., Electrospun nanofibre filtration media to protect against biological or nonbiological airborne particles. *Polymers*, (2021), 13(19)

Khatsee, S., Daranarong, D., Punyodom, W., et al., Electrospinning polymer blend of PLA and PBAT: Electrospinnability–solubility map and effect of polymer solution parameters toward application as antibiotic-carrier mats. *Journal of Applied Polymer Science*. (2018), 135(28)

Kraijic, I., El Mohsni, S., A new method for the detection of singlet oxygen in aqueous solutions. *Photochemistry and Photobiology* (1978), Vol. 28, pp. 577-581

Lawal, U., Robert, V., Loganathan, S., et al., Poly(lactic acid)/Menadione Based Composite for Active Food Packaging Application. *Journal of Polymers and the Environment*, (2023), 1938-1954, 31(5)

Li, R., Zhang, M., Wu, Y., What we are learning from COVID-19 for respiratory protection: Contemporary and emerging issues. *Polymers*, (2021), 13(23)

Liang, C., Li, J., Chen, Y., et al., Self-Charging, Breathable, and Antibacterial Poly(lactic acid) Nanofibrous Air Filters by Surface Engineering of Ultrasmall Electroactive Nanohybrids. *ACS Applied Materials and Interfaces*, (2023), 15, 57636-57648

Ma, Y., Wisuthiphaet, N., Bolt., H., et al., N-Halamine Polypropylene Nonwoven Fabrics with Rechargeable Antibacterial and Antiviral Functions for Medical Applications, *ACS Biomaterials Science and Engineering*. (2021), 2329-2336, 7(6)

Ma, Y., Huang, C., Zhang, Z., et al., Controlled Surface Radical Graft Polymerization of N-Halamine Monomers on Polyester Fabrics and Potential Application in Bioprotective Medical Scrubs. *ACS Applied Polymer Materials*, (2022), 4, 6760-6769

Muff, J., Bennedsen, L., Sogaard, E., Study of electrochemical bleaching of p-nitrosodimethylaniline and its role as hydroxyl radical probe compound. *Journal of Applied Biochemistry*, (2011), 599-607, 41(5)

Selatile, M., Ojijo, V., Sadiku, R., et al., Development of bacterial-resistant electrospun polylactide membrane for air filtration application: Effects of reduction methods and their loadings. *Polymer Degradation and Stability*, (2020), 178

Shao, W., Niu, J., Han, R., et al., Electrospun Multiscale Poly(lactic acid) Nanofiber Membranes with a Synergistic Antibacterial Effect for Air-Filtration Applications. *ACS Applied Polymer Materials*, (2023), 9632-9641, 5(11)

Sheng, L., Zhang, Z., Sun, G., Light-driven antimicrobial activities of vitamin K3 against Listeria monocytogenes, Escherichia coli O157:H7 and Salmonella Enteritidis. *Food Control*. (2020), 114

Sun, Y., Eckstein, S., Niu, X., et al., Biobased triesters as plasticizers for improved mechanical and biodegradable performances of polylactic acid fibrous membranes as facemask materials. *ACS Sustainable Chemistry & Engineering*. (2024)

Tang, P., Zhang, Z., El-Moghazy, A., et al., Daylight-Induced Antibacterial and Antiviral Cotton Cloth for Offensive Personal Protection. *ACS Applied Materials and Interfaces*, (2020)

Tian, C., Lovrics, O., Vaisman, A., et al., Risk factors and protective measures for healthcare worker infection during highly infectious viral respiratory epidemics: A systematic review and meta analysis. *Infection Control and Hospital Epidemiology*, (2022), 639-650, 43(5)

Verbeek, J., Ijaz, S., Mischke, S., et al., Personal protective equipment for preventing highly infectious diseases due to exposure to contaminated body fluids in healthcare staff. *Cochrane Database of Systematic Reviews*. (2016), 2016(4)

Wang, L., Xiong, J, et al., Biodegradable and high-performance multiscale structured nanofiber membrane as mask filter media via poly(lactic acid) electrospinning. *Journal of Colloid and Interface Science*. (2022), 961-970

Wang, S., Liang, J., Yao, Y., et al., Electrospinning-derived PLA/Shellac/PLA sandwich-Structural membrane sensor for detection of alcoholic vapors with a low molecular weight. *Applied Sciences (Switzerland)*, (2019), 9(24)

Wu, J., Liu, S., Zhang, M., et al., Coaxial electrospinning preparation and antibacterial property of polylactic acid/tea polyphenol nanofiber membrane. *Journal of Industrial Textiles*, (2022), 152808372110542

Yap, C., Lim, S., Chan, Y., et al., Potential application of menadione for antimicrobial coating of surgical sutures. *Biotechnology Notes*. (2023), 20-27, 4

Yousefimashouf, M., Yousefimashouf, R., Alikhani, M., et al., Evaluation of the bacterial contamination of face masks worn by personnel in a center of COVID 19 hospitalized patients: A cross-sectional study. *New Microbes and New Infections*, (2023), 52

Zhang, Z., Si, Y., Sun, G., Photoactivities of Vitamin K Derivatives and Potential Applications as Daylight-Activated Antimicrobial Agents. *ACS Sustainable Chemistry and Engineering*. (2019), 18493-18504, 7(22)

Zhang, Z., El-Moghazy, A.Y., Wisuthiphaet, N., et al., Daylight-induced antibacterial and antiviral nanofibrous membranes containing Vitamin K derivatives for personal protective equipment. *ACS Applied Materials and Interfaces*, (2020), 49416-49430, 12

Zhang, Z., Pan, B., Wang, L., et al., Photoactivities of Two Vitamin B Derivatives and Their Applications in the Perpetration of Photoinduced Antibacterial Nanofibrous Membranes. *ACS Applied Bio Materials*. (2021), 8584-8596, 4(12) 49442-49451, 12(44)

Zhang, Z., Wisuthiphaet, N., Nitin, N., et al., Photoactive Water-Soluble Vitamin K: A Novel Amphiphilic Photoinduced Antibacterial Agent. *ACS Sustainable Chemistry and Engineering*. (2021), 8280 8294, 9(24)

Zhao, Y., Ming, J., Cai, S., et al., One-step fabrication of polylactic acid (PLA) nanofibrous membranes with spider-web-like structure for high-efficiency PM0.3 capture. *Journal of Hazardous Materials*, (2024), 165

Chapter 4. Conclusion

This study focused on production of biobased, biodegradable, biocidal and reusable filtering materials for preparation of next generation of facemasks with improved environmental and human protection performances. The biobased and biodegradable PLA was explored as a potential replacement of petroleum-based polypropylene (PP) as face mask filtering materials. Nature based photosensitizer, menadione, vitamin K3 (VK3), was employed as photoactive agent and added into PLA, which was electrospun into light-induced antibacterial PLA-VK3 fibrous membranes. The prepared PLA-VK3 fibrous membranes were characterized and evaluated as an alternative filtration material in comparison to PP based ones. The antibacterial properties of the membranes were assessed by measurements of the production of ROS. the PLA-VK3 fibrous membranes demonstrated desired light-induced activities and antibacterial functions. However, the photo stability and activity of VK3 on fiber surfaces also caused concerns on stabilities under long-term storage and long-time light exposure, which will be addressed in following research work. The electrospun PLA-VK3 membranes also showed adequate filtration efficiency and low pressure drop allowing for a protective and breathable filtration mask to be created. The results of this study provides success of using light-induced antimicrobial agents in facemask materials, which could be useful for the development of more robust environmentally friendly and human safe and improved personal protective clothing materials.